



HAL
open science

Light absorption, light use efficiency and productivity of 16 contrasted genotypes of several Eucalyptus species along a 6-year rotation in Brazil

Guerric Le Maire, Joannès Guillemot, Otavio C. Campoe, Jose-Luiz Stape,
Jean-Paul Laclau, Yann Nouvellon

► To cite this version:

Guerric Le Maire, Joannès Guillemot, Otavio C. Campoe, Jose-Luiz Stape, Jean-Paul Laclau, et al.. Light absorption, light use efficiency and productivity of 16 contrasted genotypes of several Eucalyptus species along a 6-year rotation in Brazil. *Forest Ecology and Management*, 2019, 449, pp.1-17. 10.1016/j.foreco.2019.06.040 . hal-02629060

HAL Id: hal-02629060

<https://hal.inrae.fr/hal-02629060>

Submitted on 25 Oct 2021

HAL is a multi-disciplinary open access archive for the deposit and dissemination of scientific research documents, whether they are published or not. The documents may come from teaching and research institutions in France or abroad, or from public or private research centers.

L'archive ouverte pluridisciplinaire **HAL**, est destinée au dépôt et à la diffusion de documents scientifiques de niveau recherche, publiés ou non, émanant des établissements d'enseignement et de recherche français ou étrangers, des laboratoires publics ou privés.



Distributed under a Creative Commons Attribution - NonCommercial 4.0 International License

1 **Light absorption, light use efficiency and productivity of 16 contrasted genotypes of several**
2 ***Eucalyptus* species along a 6-year rotation in Brazil**

3 Gueric le Maire (1,2,3), gueric.le_maire@cirad.fr

4 Joannès Guillemot (1,3,4), joannes.guillemot@cirad.fr

5 Otavio C. Campoe (5,6), otavio.campoe@ufla.br

6 José-Luiz Stape (6), jlstape@gmail.com

7 Jean-Paul Laclau (1,3), laclau@cirad.fr

8 Yann Nouvellon (1,3), yann.nouvellon@cirad.fr

9 (1) CIRAD, UMR Eco&Sols, F-34398 Montpellier, France

10 (2) UNICAMP, Campinas, SP, CEP: 13083-860, Brazil

11 (3) Eco&Sols, Univ Montpellier, CIRAD, INRA, IRD, Montpellier, SupAgro, Montpellier, France

12 (4) ESALQ, Universidade de São Paulo, Piracicaba, SP, CEP 13418-900, Brazil

13 (5) Federal University of Lavras – UFLA, Lavras, MG, CEP: 37.200-000, Brazil

14 (6) UNESP-FCA, Botucatu, SP, CEP 18.610-300, Brazil

15

16 **Abstract**

17 Stemwood productivity in forest ecosystems depends on the amount of light absorbed by the trees
18 (APAR) and on the Light Use Efficiency (LUE), i.e. the amount of stemwood produced per amount of
19 absorbed light. In fertilized *Eucalyptus* plantations of Brazil, growth is expected to be strongly limited by
20 light absorption in the first years after planting, when trees can benefit from high soil water stocks,
21 recharged after clearcutting the previous stand. Other limiting factors, such as water or nutrient shortage
22 are thought to increase in importance after canopy closure, and changes in allocation patterns are
23 expected, affecting the LUE.

24 Studying changes in APAR and LUE along a complete rotation is paramount for gaining insight into the
25 mechanisms that drive the inter- and intra-genotype variabilities of productivity and stemwood biomass at
26 the time of harvest. Here, we present a 6-year survey of productivity, APAR and LUE of 16 *Eucalyptus*
27 genotypes of several species used in commercial plantations and planted in 10 randomized replications in
28 the São Paulo Region, Brazil. APAR was estimated using the MAESTRA tridimensional model
29 parameterized at tree scale for each tree in each plot (a total of 16000 trees) using local measurements of
30 leaf and canopy properties. Stand growth was estimated based on allometric relationships established
31 through successive destructive biomass measurements at the study site.

32 Allometric relationships predicting biomass of tree components, leaf surface, crown dimension and leaf
33 inclination angle distribution throughout the rotation for the 16 productive genotypes are shown. Results
34 at stand scale showed that 1) LUE increased with stand age for all genotypes, from 0.15 at age 1 yr to
35 1.70 g MJ⁻¹ at age 6 yrs on average; 2) light absorption was a major limiting factor over the first year of
36 growth (R² between APAR and stand biomass ranging from 0.5 to 0.95), explaining most of the inter- and
37 intra-genotype growth variability; 3) at rotation scale, the variability of final stemwood biomass among
38 genotypes was in general attributable to other factors than average APAR; 4) differences in stemwood
39 productions among genotypes remained large throughout the rotation; 5) LUEs over the second half of the
40 rotation, rather than initial growth or APAR, was the major driver of stemwood biomass at the time of
41 harvest.

42 **Keywords:** eucalypt clone, light interception, productivity, tropical plantation, production ecology, leaf
43 area index

44 1. Introduction

45

46 In recent years, trade of wood products has increased sharply in response to the growing demand for
47 industrial wood (e.g. particle board), paper and cardboard, coal for industry (e.g. iron and steel), among
48 other products. This increase in wood demand is expected to strengthen in the future (+20% by 2060,
49 Elias and Boucher (2014)). Given the depletion of the natural forest resources, the area of productive
50 forest plantations has sharply increased (Elias and Boucher, 2014). Planted forest areas increased from
51 168 to 278 million hectares between 1990 and 2015 (FAO, 2015; Keenan *et al.*, 2015; MacDicken, 2015).
52 Forest plantations are providing an increasing share of the world's wood products, representing 6.9% of
53 total forest area in 2012 (1.8% in South America), but responsible for 46.3% of the roundwood
54 production (89.8% in South America) (Payn *et al.*, 2015). Under appropriate policies and market
55 regulations, commercial forest plantations are one of the options to tackle the current global forest
56 degradation and deforestation by substituting wood products from natural forests (Pirard *et al.*, 2016).

57 *Eucalyptus* plantations account for 33% of tropical forest plantations, with *ca.* 20 Mha planted worldwide
58 (Iglesias-Trabado *et al.*, 2009). In 2016, *Eucalyptus* plantations covered 5.67 Mha in Brazil, mostly for
59 industrial use and located in the southern half of the country (IBA, 2017). The average production of
60 *Eucalyptus* plantations in Brazil is 35.7 m³ ha⁻¹ year⁻¹, managed in rotations of 6 to 8 years (IBA, 2017).
61 With gross primary productivity (GPP) of about 4.2 kg C m⁻² yr⁻¹ and net primary productivity (NPP) of
62 up to 3 kg C m⁻² yr⁻¹ (Stape *et al.*, 2008; Ryan *et al.*, 2010; Nouvellon *et al.*, 2012; Epron *et al.*, 2013),
63 these planted forests rank among the most productive ecosystems in the world (Luysaert *et al.*, 2007).

64 Large disparities do exist, however, with observed productivities ranging from 20 to 60 m³ ha⁻¹ year⁻¹
65 among plantations, as a result of contrasting pedoclimatic conditions, genetic material and management
66 (Gonçalves *et al.*, 2013; Binkley *et al.*, 2017). To reach the highest productivities, local genetic
67 improvement through breeding programs have been conducted in the main *Eucalyptus* cultivation areas of
68 Brazil, aiming to increase adaptation to different environmental contexts. *Eucalyptus* species or hybrids
69 are planted in a rainfall range from 500 to 2000 mm and an average annual temperature range from 19 to
70 27 °C (ABRAF, 2012).

71 Breeding programs are primarily focused on production performance and wood quality at the time of
72 harvest, which integrates *de facto* genetic potential, and its interaction with management, pedoclimatic
73 conditions and resistance to biotic and abiotic stresses. Building on the high diversity of resource
74 acquisition and ecological strategies found among *Eucalyptus* species and provenances (Drake *et al.*,
75 2015; Pfautsch *et al.*, 2016; Aspinwall *et al.*, 2019) the genetic materials currently in use display a broad
76 range of physiological, structural, biochemical and life history traits (Gonçalves *et al.*, 2013). However,
77 the biological mechanisms and associated traits responsible for the differences in final trunk biomass
78 production and wood quality remain unclear, mostly because of the high covariation commonly observed
79 among traits (Reich, 2014). Process-based models calibrated using local measurements of functional traits
80 and evaluated against carbon and water cycling data have proved useful to untangling the mechanisms
81 responsible for forest productivity (Marsden *et al.*, 2013; Christina *et al.*, 2015; Guillemot *et al.*, 2015).
82 Furthermore, the variability of soil and climate conditions occurring at both local and regional scales
83 affects the intra-genotype variability of productivity, which hinder the quantification and analyse of inter-
84 genotype variability. Performance comparisons among genotypes are therefore conducted in forestry trials
85 that aim at controlling the variability attributable to soil and residue management (Gonçalves *et al.*, 2007;
86 du Toit *et al.*, 2010), fertilization (Laclau *et al.*, 2009), water supply (Stape *et al.*, 2008), rainfall exclusion
87 (Battie-Laclau *et al.*, 2014), stocking (Stape and Binkley, 2010; Crous *et al.*, 2013; Resende *et al.*, 2018),
88 genotypes (Pallett and Sale, 2004; Silva *et al.*, 2016) or a combination of these effects (Binkley *et al.*,
89 2017).

90 Large differences in leaf size, foliage area per tree, spatial distribution of leaf area within the canopy, leaf
91 inclination angles, optical properties and crown dimensions are observed among genotypes, resulting in
92 different light absorption capacities. Light absorption capacity is thought to be a major factor limiting
93 growth at tree scale across a broad range of environmental contexts and management (Binkley *et al.*,
94 2010; Binkley *et al.*, 2013; Campoe *et al.*, 2013). At stand scale, however, the positive effect of light
95 absorption on GPP and biomass production (Russell *et al.*, 1989; Wang *et al.*, 1991; Will *et al.*, 2001) can
96 be obscured by other limiting factors (Landsberg and Waring, 1997). For instance, Marsden *et al.* (2010)

97 showed that the total absorbed radiation (APAR) was well related to productivity among stands planted
98 with the same *Eucalyptus* genotype in the first two years after planting, but vanished afterward. One
99 reason could be the influence of water deficit on tree growth which is much larger after canopy closure
100 (Christina *et al.*, 2017; Christina *et al.*, 2018). The effect of light absorption on forest productivity is also
101 expected to vary among genotypes, soil, climate and management conditions (Forrester *et al.*, 2018).
102 Heterogeneity within a stand was shown to partly explain differences in production for a given genotype,
103 higher heterogeneity reducing significantly the productivity (Binkley *et al.*, 2010; Ryan *et al.*, 2010; Stape
104 *et al.*, 2010; Luu *et al.*, 2013). Heterogeneity could also explain differences of production observed
105 among genotypes, e.g. if some genotypes show more tendencies towards heterogeneity and competition
106 than others (Resende *et al.*, 2016; Soares *et al.*, 2016; Resende *et al.*, 2018).

107 The present study aims at exploring the age-related changes in APAR, and the relationship between light
108 absorption and stemwood production across 16 contrasted *Eucalyptus* genotypes at stand scale. In other
109 words, our main objective is to test whether differences in stem production among genotypes are mostly
110 related to differences in APAR or to differences in the light use efficiency for stemwood production
111 (LUE), or both. The following specific questions are addressed:

- 112 - What are the changes of tree growth and APAR along the rotation?
- 113 - Which traits explain the differences in APAR among genotypes (e.g. leaf area index, leaf optical
114 properties, leaf inclination angles or canopy clumping)?
- 115 - How does LUE vary among genotypes, and how does it correlate with annual growth?
- 116 - Does within-stand heterogeneity of tree sizes explain the variability of production among clones?
- 117 - How do the drivers of stemwood production change across a local gradient of soil properties?

118

119 Sixteen genotypes from different origins were compared in a randomized block design set up at a single
120 site in the field, in order to reduce the effects of changes in soil, climate and management on the inter-
121 genotype comparisons. The studied genotypes were selected among the most productive ones from the
122 South to the North of Brazil. Each selected genotype has good performances in some pedo-climatic
123 conditions of Brazil, but these conditions do not necessarily correspond to the local conditions of the field
124 trial in our study. This was expected to lead to a large range of wood productivity, and thus useful to gain
125 insight into the mechanisms underlying genotype performances.

126

127 **2. Material and Methods**

128

129 2.1. Study site and experimental design

130 The experiment was set up within a commercial plantation of 90 ha located in the State of Sao Paulo,
131 south-eastern Brazil, at 22°58'04''S and 48°43'40''W, 750 m.a.s.l. and managed by the EUCFLUX
132 project, from the Forestry Science and Research Institute (<http://www.ipef.br/eucflux/en/>). It consisted in
133 10 repetitions (blocks) of 16 plots (Figure 1a), each plot being planted with one different *Eucalyptus*
134 genotype (G1 to G16, Table 1). Each block was made of a 4x4 grid of 16 plots where genotypes were
135 randomly distributed (Figure 1b). Each plot was planted with a single genotype with a tree spacing of 3x2
136 m (1666 trees ha⁻¹). Each plot was 36x32 m large and contained 12 lines of 16 planted trees. Only the 100
137 central trees are studied to avoid border effects between plots. An entire block had therefore a size of
138 144x128 meters. All blocks were managed following the standards currently used by Brazilian *Eucalyptus*
139 plantation companies (Gonçalves *et al.*, 2013) throughout the entire rotation. The experiment was planted
140 in November 2009. The mean annual rainfall was 1430 mm y⁻¹ over the study period, 85% of this amount
141 occurring between October and May, which is the period with high incoming global radiation (Christina
142 *et al.*, 2017). The 10 blocks were distributed over the 90 ha commercial plantation, which topography was
143 mostly flat, excepted some slight declivity in the North-western and North-eastern parts of the area, down
144 to a small river (see the riparian natural vegetation on Figure 1a). The soil was a deep Ferralsol over the
145 whole area but the slight declivity was associated with a gradual change in soil texture properties
146 (Campoe *et al.*, 2012), from sandy soils upward (including blocks B1 to B7) to more clayish soils
147 downward (blocks B8, B9 and B10). A complete physical and chemical description of the soil profile was
148 performed in Pinheiro *et al.* (2016). A long-term ecosystem observatory at the center of the 90 ha stand,
149 was equipped with a complete meteorological station and an Eddy-covariance tower (Nouvellon *et al.*,
150 2010; Christina *et al.*, 2017; Nouvellon *et al.*, 2018). We surveyed the experiment for 6 years, which
151 corresponds to the standard rotation duration of commercial *Eucalyptus* plantations for industrial
152 roundwood in Brazil.

153

154 2.2. Stand inventories

155 All trees of the inner plots were individually surveyed for diameter at breast height (DBH) and tree height
156 (H). DBH measurements were made at 8 dates in all blocks (i.e. 100 trees x 16 plots x 10 blocks = 16,000
157 trees), and at 5 additional dates in a subset of blocks (Table 2). H measurements were made on all trees
158 during the first two years and on a subset of 24 central trees per plot afterwards (Table 2). Power
159 relationships between measured DBH and H were established on these 24 trees to estimate H for the non-
160 measured trees. DBH of all border trees were measured twice during the 6 years, and their values for

161 other dates were obtained using between-date relationships calibrated on the inside plot measurements of
162 the same genotype and same block. H of border trees was then computed using DBH-H power
163 relationships calibrated on measurements in the inner plot at the same date. Finally, tree DBH and H in
164 the plots (including border trees) were linearly interpolated at daily time step, for each tree and for the 6
165 years. The percentage of dead trees was recorded at each inventory date (hereafter called “mortality”).
166 The GINI Index was also computed: this heterogeneity index can be used to evaluate the within plot
167 competition between trees, using distributions of tree basal areas. It is based on the Lorenz curve and
168 proved to be efficient at quantifying differences in stand structures among diverse forest management
169 systems (Cordonnier and Kunstler, 2015; Fernández-Tschieder and Binkley, 2018). It was computed
170 using the *lorenz.curve* function of the *lawstat* package of R software (v3.5.1). The higher the index, the
171 more competition among trees.

172

173 2.3. Tree biomass measurements

174 Destructive sampling of trees for biomass, leaf area, crown dimensions, leaf angles, and leaf optical
175 measurements were performed at 5 dates over the 6-year survey (Table 2) in all genotypes. At each date,
176 12 trees per genotype were sampled. Sampled trees were distributed among blocks (Table 2) and selected
177 to encompass the DBH range measured in the inventories, which is the method generally adopted for
178 these eucalypt plantations (Laclau *et al.*, 2008). Only border trees were cut to avoid as much as possible
179 perturbations and changes in tree growth in the inner plots.

180 After felling the tree, the height of the crown base and crown length was measured. The tree was then cut
181 at crown base, the crown was straighten up vertically to measure leaf angle and crown radius (in the row
182 and inter-row directions). Note that felling the tree did not damage the crown. Leaf angle distributions
183 were measured on these 12 sampled trees per genotype. In each tree, 72 leaves were selected for angle
184 measurement as follows: at three heights in the canopy, four axillary branches were randomly selected
185 among the four azimuthal quarters, two of them in the row direction and the other two in the inter-row
186 direction. Six leaves were randomly selected between the basis and the end of each branch. On each leaf,
187 the vertical component of the leaf blade’s inclination was measured with a clinometer. The leaf angle
188 distribution (LAD) was obtained at 10° intervals for each genotype and each date.

189 Felled tree compartments were then weighted in the field, separating trunk (diameter > 2 cm at the
190 thinnest end), living branches, dead branches and leaves. Subsamples of stemwood, bark and branches
191 were taken to the laboratory and weighted before and after drying until constant weight. For leaf biomass,
192 the green crown length of felled trees was divided into three equal-length sections (lower, middle and

193 upper). All leaves were weighted immediately after tree fall for each section. Twenty-five leaves were
194 randomly selected for each crown section and kept cold until their fresh mass and area were measured in
195 the laboratory. Trunk, bark, branch and leaf subsamples were then dried at 65 °C until constant weight.
196 Average dry matter content (ratio of the sample dry mass over the fresh mass) were calculated for each
197 tree and combined to field-based fresh weight to calculate the dry biomass of all tree components. The
198 leaf area of each crown section was calculated by multiplying the total field-based fresh mass by the leaf
199 area to fresh mass ratio (calculated on the 25 sampled leaves). Single-tree leaf area and leaf biomass were
200 computed by summing the values of each crown sections.

201 We measured the optical properties of leaves of each genotype at 1 and 6 years of age in two different
202 blocks (Table 2) in 3 trees of different size, with 6 leaves measured per tree (3 crown sections * 2
203 samples), totalizing 1152 single leaf measurements. The reflectance and transmittance of these leaves
204 were measured in the visible and near infrared spectra with an ASD FieldSpec Pro (Analytical Spectral
205 Devices, Boulder, Colorado, USA) spectrometer and a Licor integrating sphere (Oliveira *et al.*, 2017).
206 SPAD measurements, which are highly correlated with leaf chlorophyll content per unit of leaf area, were
207 performed on the same leaves with the Chlorophyll Meter SPAD-502 (Minolta Camera, Osaka, Japan),
208 averaging 5 to 10 SPAD readings per leaf. A supplementary SPAD measurement was done at 4.6 years of
209 age (Table 2).

210

211 2.4. Allometric relationships calibrations

212 After having tested many forms of age-related allometric equations issued from Saint-André et al (2005)
213 and Picard et al. (2015) (not shown), we found that Equation (1) was the most precise and flexible to
214 predict trunk and living branch biomass:

$$215 Y = a * age^b * D2H^{c*age^d} \quad \text{Eq. 1}$$

216 Where Y is the variable to predict (trunk or branch biomass). D2H is the product of squared DBH (m²)
217 and H (m), *age* is the age of the trees (in years as in Table 2), *a*, *b*, *c* and *d* are parameters to be estimated.
218 Parameters were fitted using the *nls* function of R software. For a given genotype, we tested two fit
219 options: one with the data from all blocks, and another including a “site” effect, i.e. fitting two different
220 equations, one for blocks B1 to B7 (sandy blocks) and another for B8 to B10 (clayey blocks, Fig. 1).
221 Model selection was based on Akaike Information Criterion (AIC).

222 For leaf area and leaf biomass, a genotype-specific allometric relationship was calibrated at each
223 inventory date (without age effect), with the following equation:

224 $Y = a * X^b$ Eq. 2

225 Where Y is the variable to predict (leaf area or leaf biomass), and X is either DBH or D2H. As before, a
226 model selection procedure based on AIC was used to select the best predictor (DBH or D2H) and select
227 between one common equation for all blocks or two different equations for sandy and clayey blocks.

228 After applying the final allometric equations to each tree measured at each inventory date, Leaf Area
229 Index (LAI, $m^2_{leaf} m^{-2}_{soil}$) was computed by summing the calculated tree leaf area of all trees within each
230 plot and dividing the result by the plot areas. Specific Leaf Area (SLA, $m^2 kg^{-1}$) was obtained by dividing
231 the total leaf area of the plot by the sum of the tree leaf biomass of all trees of that plot. Time
232 interpolation of tree leaf area between the inventory dates was done following the methodology adopted
233 in other studies, using remote-sensing data to account for the seasonal dynamics of tree leaf area and LAI
234 (le Maire *et al.*, 2011; le Maire *et al.*, 2013; Christina *et al.*, 2017).

235 Other allometric relationships were calibrated to estimate tree dimensions needed for MAESTRA model
236 simulations: crown diameter (D) in the directions of the planting row and the inter-row (Equation 3) and
237 the crown ratio (CR), which was the ratio between the crown height and the total height of the tree (Eq.4).
238 Single equation per genotype for all blocks and using DBH had systematically lower AIC.

239 $D = a * age^b * DBH^{c*age}$ Eq. 3

240 $CR = a * age^b * (DBH + c)$ Eq. 4

241 Finally, the dependency of Leaf Inclination Angle (LIA) to height was explored. Leaf angles are indeed
242 commonly observed to vary along a vertical gradient in forests, from sun leaves on the top of the canopy
243 having large angles to more horizontal leaves at the bottom of the canopy (Russell *et al.*, 1989; Posada *et*
244 *al.*, 2009). From destructive measurements, average leaf angle per section of crowns (three sections: top,
245 middle and bottom) was associated to the central height of this crown section. The following equation
246 was fitted for each genotype:

247 $LIA = a * age^b * H_m^{age^c}$, Eq. 5

248 where H_m was the measurement height, i.e. the height from the soil to the middle of the crown section
249 where the angles of the leaves were measured. The standard deviation of LIA was constant across
250 measurement height.

251

252 2.5. Simulations of fAPAR, Extinction Coefficient, and LUE

253 The MAESTRA processed-based model (Medlyn, 2004) is an improvement of the MAESTRO model
254 (Wand and Jarvis 1990). The light interception calculation is based on Norman and Welles (1983) and is
255 described in other studies (Wand and Jarvis 1990, Medlyn 98, Bauerle 2004). The MAESTRA model has
256 been applied in many other studies dealing with *Eucalyptus* plantations (Campoe *et al.*, 2013; le Maire *et*
257 *al.*, 2013; Christina *et al.*, 2016; Christina *et al.*, 2017; Christina *et al.*, 2018; Vezy *et al.*, 2018), and a
258 detailed description of the model and parameterization for different *Eucalyptus* plantations can be found
259 in these studies.

260 The model was parameterized for the 16 genotypes in all 10 blocks (Figure 1b). For each block, all trees
261 were described in the model, including border trees in all the plots. Parameters at tree level were: position
262 in the plot (x,y), height, crown height, crown radius in the row and inter-row directions and leaf area,
263 which were obtained by applying the allometric equations (Section 2.4) to tree inventories. Leaf
264 inclination angle distribution was computed at plot scale, for each genotype, block and date, after having
265 applied the Equation (5) to all crown sections of all trees of the inventories and weighted by their section
266 leaf areas. Other parameters such as reflectance and transmittance of leaves were averaged at genotype
267 level, and linearly interpolated between measurements dates. The same horizontal distribution of leaf area
268 density within crowns were used for all genotypes, because no local measurements were available (values
269 from Christina *et al.* (2016) in a neighbouring stand). Meteorological data used in these simulations
270 consisted in half-hourly gap-filled (only 0.15 % of missing data) global radiation converted to
271 Photosynthetically Active Radiation (PAR), that was measured on top of the eddy-covariance tower
272 (Figure 1a) during the entire simulation period.

273 Simulations were performed at half-hourly time-step, in all inside plots of all blocs (i.e. for 16,000 trees).
274 To speed-up the computation time, we chose to perform simulations of one day every 20 days. The ratio
275 of the sum of the radiation absorbed by all within-plot trees (APAR) to incident PAR is the fraction of
276 absorbed PAR (fAPAR). Daily fAPAR was computed for these simulated days and interpolated in time
277 for each plot. Daily APAR of non-simulated days were estimated as the product of interpolated fAPAR
278 and the incident PAR. Annual values of fAPAR were also computed as the annual sum of APAR divided
279 by annual sum of incident PAR.

280 As PAR absorption is influenced by many canopy structural parameters other than LAI (crown size and
281 shape, LIA, Leaf optical properties, etc), we computed effective extinction coefficients for daily PAR
282 absorption in order to assess the overall effect of these parameters. Extinction coefficients (k) were

283 computed for each plot with a non-linear regression of the following simplified and widely used equation
284 (Landsberg and Hingston, 1996; Almeida *et al.*, 2004), for each year:

$$285 \quad fAPAR = 1 - \exp(-k * LAI) , \quad \text{Eq. 6}$$

286 where fAPAR is the fAPAR computed over the annual period and LAI is the averaged LAI at the same
287 dates.

288 APAR was further used to compute the light use efficiency for NPP of stemwood (LUE, g MJ⁻¹):

$$289 \quad LUE = \frac{NPP_{stem}}{APAR} , \quad \text{Eq. 7}$$

290 where NPP_{stem} (g m⁻² y⁻¹) is the annual Net Primary Production of stemwood biomass at plot level.
291 NPP_{stem} is different from the stemwood biomass variation (ΔB). ΔB is computed as final minus initial
292 living stem biomass during a time period, and is further used in the manuscript as “stemwood biomass
293 growth”. NPP_{stem} is the sum of ΔB and the biomass of trees that died during the same time period.
294 APAR is the total PAR absorbed by the plot during the same period. Growth Efficiency (GE, g m_{leaf}⁻² y⁻¹),
295 also called Leaf Area Efficiency, was similarly computed as the ratio of NPP_{stem} and LAI.

296

297 2.6. Model validation

298 Simulated APAR is difficult to validate against measurements, since APAR cannot be measured easily on
299 a large number of plots. Instead, as in other studies (Charbonnier *et al.*, 2013; le Maire *et al.*, 2013;
300 Christina *et al.*, 2015), we validated another simulated intermediate variable, which is of high importance
301 in the APAR simulation: the gap fractions (GF) as a function of view angles. We compared the measured
302 and simulated directional GF at ground level, as in Rouspard *et al.* (2008). Canopy structures strongly
303 varied among genotypes, as illustrated with vertical upward pictures in Figure 2, which allowed testing
304 the MAESTRA model on a large range of light interception conditions.

305 Measurements of directional gap fractions (GF) were conducted using two LiCor PCA LAI-2000 (Li-Cor,
306 Lincoln, NE, USA) on June 2014, in all plots of blocks B2, B3 and B8 (Table 2). In each plot, 12
307 measurements were made below the canopy with one LAI-2000 device using a 180° azimuthal field of
308 view, with the viewing direction parallel to planting lines, in periods with *ca.* 100% diffuse incoming
309 light. The locations of the measurements were distributed in a systematic grid to cover a large part of the
310 plot and to sample points at different distances from the trees but never in front of a tree trunk (see
311 positions in Figure 1b). Continuous measurements of incident radiation were performed simultaneously at
312 the top of the central tower with the second LAI-2000, which was inter-calibrated with the first one and

313 which used the same measurement configuration (orientation and view cap). The ratio between below-
314 and above-canopy measurements were computed for the five zenithal rings of the LAI-2000 fish eye lens
315 and were used as an estimate of the directional gap fraction. Simulated GF at the same locations, angles
316 and date were obtained from MAESTRA simulations. The simulated and measured angular GF values
317 were then averaged per genotype and compared. The Diffuse Non-Interceptance (DIFN) values,
318 computed as in the LAI-2000 manual (LI-Cor, 1992), were compared between simulations and
319 measurements. The value of (1-DIFN) is a good proxy of the APAR of the canopy under diffuse
320 conditions, even though leaf reflectance and transmittance and soil reflectance may affect the
321 correspondence between both variables.

322

323 2.7. Statistical analysis

324 Half-hourly tree-scale simulations of MAESTRA were averaged over each plot (i.e. 10 plots for each of
325 the 16 clones), and each year. As described before, the simulations were averaged annually, for each
326 growing year. Statistical analyses were performed on variables that were all averaged over the same time
327 periods. The analysis of observations and MAESTRA simulations were conducted using Pearson
328 correlations and linear mixed models (*lmer* function of *lme4* package of R). A linear mixed model
329 between fAPAR and variables described in Table 3 was computed at each age, including blocks as
330 random effect. We first performed a model selection based on the Variance Inflation Factors (VIF) in
331 order to deal with multicollinearity among variables. Variables having highest VIF were iteratively
332 removed one by one until all remaining variables had a VIF lower than 5. Then, we performed a simple
333 backward elimination of non-significant effects of the linear mixed effects model, starting with the
334 remaining variables after VIF elimination (*step* function of *lmerTest*). Final model F-test of fixed effects
335 are computed using the Satterthwaite's method. Another more simple linear mixed models was computed
336 between annual stemwood growth and genotype, APAR, GINI and blocks, with blocks as random effects.
337 Fraction of variation attributable to each variable in regression model were computed using the
338 *calcVarPart* function of the *variancePartition* package. Least Significant Difference (LSD) used in
339 graphical representation of inter-genotype difference was computed using the *LSD.test* function of
340 package *agricolae*.

341 3. Results

342 3.1. Time course of the characteristics of each genotype in each plot

343 *Allometric relationships*

344 Allometric relationships predicting the biomass of tree components throughout the rotation for highly
345 productive genotypes used in commercial plantations are illustrated in Figure 3 for genotype 14, and
346 figures and equations for all other genotypes are given in *Supplementary Material 1 “allometric*
347 *relationships”*. Most of the relationships had high r-square and low Root Mean Square Error, allowing a
348 precise estimation of single tree characteristics for all ages, genotypes and blocks. For some genotype,
349 using distinct allometric equations for sandy (B1-B7) and clayey (B8-B10) areas yielded better fit of
350 trunk and branch biomass. For tree leaf area (and therefore LAI and SLA), the allometric relationships
351 changed between the sampling dates.

352 *Leaf area index*

353 The average annual LAI increased during the first 2 years, to reach a peak value during the second year,
354 and then decreased until the end of the rotation (Figure 4). The temporal evolution along the rotation was
355 mostly similar among genotypes. Large differences in LAI were observed the second year after planting
356 between genotypes, up to $3 \text{ m}^2 \text{ m}^{-2}$. The genotype G16 showed the lowest LAI throughout the rotation,
357 averaging $3 \text{ m}^2 \text{ m}^{-2}$ (reaching a peak value of $4.2 \text{ m}^2 \text{ m}^{-2}$ at 2.6 years old, data not shown), while the
358 genotype G11 had the highest average LAI of $4.5 \text{ m}^2 \text{ m}^{-2}$ (and a peak value of $6.5 \text{ m}^2 \text{ m}^{-2}$ at 2.6 years old,
359 data not shown). The LAI of the other genotypes were quite homogeneously distributed between these
360 extremes, and differences between genotypes were significant each year. A seasonal decrease in LAI
361 during the cold and dry season was observed in the data (data not shown). SLA decreased with age for
362 almost all genotypes as observed in other works (Sands and Landsberg, 2002; Almeida *et al.*, 2004; le
363 Maire *et al.*, 2011), and particularly for the seed origin G1 and G2 (Supplementary Material 4).

364 *Trunk biomass and tree growth*

365 The time course of biomass of the stem, branch and leaves is presented in Figure 4. Stem biomass almost
366 linearly increased during the 6 years of the rotation (Figure 4). The pattern was totally different for the
367 biomass of living branches and leaves, which reached a plateau (branch biomass) or slightly decrease
368 (leaf biomass) from the 3rd year to the 6th year after planting. Branches and leaves therefore accounted for
369 a decreasing percentage of the total aerial living biomass, from 20% at the end of the third year to 5% at
370 the end of the rotation.

371 The differences in stem biomass among genotypes at the end of the 6-year survey were very large and
372 highly significant. For instance, the biomass of G10 (21.5 kg m^{-2}) was on average across the 10 blocks
373 35% higher than that of G15 (15.9 kg m^{-2}) at age 6 years (Figure 5). Between these extremes, the 16
374 genotypes were fairly well distributed, some being significantly different from the others whatever stand
375 age (Figure 4 and Figure 6). However, their ranking changed along the rotation, with some genotypes

376 such as G8 or G16 starting with a very strong growth until the fourth year, but then slowing down, while
377 other genotypes (e.g., G5 and G10) steadily accumulated stem biomass throughout the rotation (Figure 4).
378 Some genotypes, such as G9, exhibited a large difference in plot biomass and productivity among blocks,
379 which tended to increase toward the end of the rotation due to outliers with low values (Figure 4). This
380 was mostly due to an increase in tree mortality in some of their plots (Figure 4 and 6).

381 *Mortality and intra-plot competition*

382 Mortality was generally low in the experiment, most genotypes having less than 5% of dead trees
383 compared to stocking at planting, on average, at the end of the rotation (Figure 4 and 6). However,
384 mortality was significantly different among genotypes, some genotypes (e.g., G1, G2, G3 and G13) being
385 more severely affected than others. G1 and G2 were from seed origins and had higher number of dead
386 trees since the first year of the rotation, while genotypes G3 and G13 displayed high mortality rates,
387 possibly caused by a sensitivity to extreme wind. Some particular events occurred at some plots, such as a
388 lightning strike, pathogen attack and other causes of tree dieback. Some blocks, such as B2, but more
389 clearly B10, showed high mortality rate for all genotypes.

390 Competition among trees within plots is both the result of differences in tree development and spatial
391 heterogeneity created by mortality of some trees. GINI heterogeneity index showed that the level of
392 competition was in general low ($GINI < 0.25$) (Cordonnier and Kunstler, 2015; Fernández-Tschieder and
393 Binkley, 2018). Competition intensity, as captured by Gini index, differed among genotypes: all
394 genotypes followed a comparable trajectory with time, but at different absolute levels. The four genotypes
395 showing the highest competition level also showed the highest mortality rates, and the highest
396 heterogeneity in tree height (Figure 4). As expected, the two seed-origin genotypes (G1 and G2) had the
397 highest GINI index. The GINI index decreased from the first to the second year, and then increased
398 steadily with time for all genotypes. Standard deviation of tree height also increased along the rotation,
399 meaning that tall tree grew faster in height than smaller ones.

400 *Leaf angles distributions and optical properties*

401 Leaf inclination angle distributions were highly variables among genotypes and changed with time along
402 the rotation. Illustration for two contrasted genotypes, G6 and G16 are given in Figure 7, and figures and
403 equations for all other genotypes are given in *Supplementary Material 2 "Leaf inclination angle*
404 *distributions"*. Some genotypes had erectophile-like leaf angle distribution, such as the G14 or G16,
405 while others tended to be more planophile (e.g. G3, G6). Changes of LIA with time was significant for
406 some genotypes, progressively changing from a planophile-like distribution at young ages to more
407 erectophile leaves (e.g. G1, G2, G3, G6, G8, G15). Other genotypes, on the contrary, did not show large

408 changes of LAD with time (e.g. G4, G9, G10, G16). All genotypes showed a clear leaf inclination change
409 from the top to the bottom of the canopy, with more erectophile leaves at the top and more planophile
410 leaves at the bottom (see Figure 7 and Supplementary Material 2). It is interesting to note that this trend is
411 found in all trees, whatever their size within the canopy: top leaves of a small tree have similar angles
412 than bottom leaves of tall trees.

413 The reflectance and transmittance of leaves were not statistically different between genotypes due to high
414 within-genotype variability of leaves within the crown. The observed increase of SPAD values between
415 age 1 and 6, for almost all genotypes (Figure 8 and Supplementary Material 4), is coherent with the
416 decrease of reflectance and transmittance, which was accounted for in the light transfer simulations.
417 SPAD values increased for almost all genotypes, and inter-genotype differences were high.

418

419 3.2. Validation of the light transfer modelling

420 Measured and modelled directional gap fractions were in close agreement for much of the genotypes
421 (Supplementary Material 3 “MAESTRA validation”, Figure SM3.1). There were substantial differences
422 in gap fraction among genotypes, as visually observed in the field on the day of the measurements (Figure
423 2), which was well captured by the model. The vertical GF was more difficult to simulate accurately,
424 because this angle integrated small canopy areas and was therefore more subject to uncertainties in tree
425 positions and sizes, but the agreement between simulations and measurements is correct. The shape of the
426 decrease of GF with view angle is related to the leaf angle distributions and dimensions and locations of
427 the crowns and was also well simulated for most of the genotypes.

428 When comparing the simulated and measured (1-DIFN) variables, the correlation was high (Pearson
429 correlation $r=0.84$, $p<0.001$) and the results were good for the three blocks where the measurements were
430 carried on (Supplementary Material 3, Figure SM3.2). The results were slightly underestimated for high
431 values and overestimated for low values. Large differences in (1-DIFN) among genotypes were well
432 captured, which confirmed that the MAESTRA model was able to simulate APAR in contrasting stand
433 structures.

434

435 3.3. Genotype differences in APAR and fAPAR

436 fAPAR increased rapidly during the first two years, and then reached a plateau with values between 0.8
437 and 0.97 (Figure 4). From the second year on, APAR interannual variation was therefore mostly driven by

438 changes in average annual incident PAR. The increase in fAPAR at the beginning of the rotation mostly
439 resulted from the increase in LAI and crown diameter and height. A saturation of fAPAR when LAI
440 reached approximately $3 \text{ m}^2 \text{ m}^{-2}$ was observed for all genotypes along the rotation (Figure 4). Variations
441 of fAPAR also resulted from other structural characteristics of the canopies taken into account in the
442 MAESTRA modelling, such as crown size and shape, leaf inclination angle distribution, leaf distribution
443 within crowns, and leaf optical properties. All these variations were summarized in the Extinction
444 Coefficient variable (Figure 8 and *Supplementary Material 4*). Extinction coefficient showed an initial
445 decrease until 3 years of age, followed by an increase, and large differences between genotypes. A simple
446 mixed model predicting stem growth in function of the genotype and APAR and their interactions, with
447 blocks considered as random effects, showed that APAR and genotype were always significant predictors,
448 but that their interactions occurred only in the first four years (data not shown). So in the first years, the
449 Growth vs. APAR relationship changed among genotypes, but the genotype principal effect on stem
450 growth subsequently become stronger and independent of APAR.

451 A linear mixed model of fAPAR in function of plot averages characteristics, with all genotypes included
452 and with the blocks considered as random effect, confirmed the highly significant importance of LAI all
453 along the rotation (Table 3). LIA was also significantly affecting fAPAR all along the rotation, except for
454 the 5th and 6th year. Plot average height significantly affected fAPAR along the rotation. Mortality had a
455 significant effect in the 4th year only, when several genotypes suffered from high mortality increase
456 (Figure 6), which created gaps only partly compensated by increasing growth of neighbour trees. Finally,
457 average optical properties were significant at explaining the inter-plot variations of fAPAR at the end of
458 the rotation.

459 3.4. Genotype differences in Growth Efficiency and LUE

460 Growth efficiency (GE), a measure of the amount of stemwood produced per year and per unit of leaf
461 area, was in general increasing along the rotation (Figure 4). The GE variability among genotypes was
462 very high and significant, with some genotypes such as G16 having a very high GE at the beginning of
463 the rotation that stabilized with stand age, while other genotypes had lower GE at the beginning but it
464 increased steadily to reach high values at the end of the rotation (e.g., G10).

465 Similarly to GE, light use efficiency for stemwood production (LUE) increased during the rotation.
466 However, some differences appeared between GE and LUE: the genotypes having high GE did not
467 necessarily showed high LUE. These differences resulted from the non-proportionality between LAI and
468 fAPAR (see section 3.3). The slight decrease observed in LUE in the 5th year was mostly due to the slight
469 increase in APAR during that year, which did not impact tree growth. This increase of APAR was mostly

470 attributable to an increase in annual incoming PAR. Despite being affected by inter-annual changes in
471 growth conditions, the LUE showed a slightly increasing trend, consistent along the rotation. fAPAR was
472 indeed almost constant for most of the rotation, while trunk growth slightly increased. Rotation averaged
473 LUE, shown in Figure 9 c, show high difference among genotypes, with 29% higher value for G10 (1.35
474 g MJ⁻¹) than for G2 (1.05 g MJ⁻¹).

475

476 3.5. Drivers of the spatial variability of trunk growth in function of stand age and genotypes

477 Variability in LAI and APAR among genotypes did not explain variability in production (Figure 9 a, b)
478 summed over the entire rotation. By contrast, the inter-genotype variability of LUE explained a large part
479 of the variability in productivity (Figure 9c). In other words, genotypes with higher LAI, or absorbing
480 more radiation along the rotation, did not systematically produce more stemwood. Other processes than
481 light absorption, captured in the Light Use Efficiency for stemwood production, were responsible for
482 differences in productivity among genotypes. However, LAI and APAR explained the spatial differences
483 (inter-block) in stemwood production of some genotypes (e.g., G7 and G13, Figure 9 d, e). On an annual
484 basis, the correlation was especially high and significant in the first year of the rotation, when the net
485 primary production of stemwood was highly linearly related with APAR (Figure 10). In the first year,
486 APAR explained most of the spatial variation of stemwood production. This production was however
487 very low compared to subsequent years. From the second year on, some genotypes were more responsive
488 to change in their APAR (e.g., G10 and G14) than others. The absence of a significant APAR-growth
489 relationship was likely due to the absence of inter-block variability of APAR (e.g., G5), or of stemwood
490 growth (e.g., G9). LUE explained most of the spatial variability of stemwood production (Figure 9 f).
491 This was expected in this context since LUE was computed as the part of the productivity that was not
492 directly explained by absorbed PAR. To summarize, the variability of wood production was primarily
493 attributable to differences among genotype that were not captured by differences in APAR all along the
494 rotation (Figure 11). APAR significantly explained growth differences among genotypes in the first year,
495 in the fourth and at the end of the rotation, while GINI competition index (within-plot competition
496 intensity) was observed to have a substantial effect at the middle of the rotation (from 2nd to 4th years). The
497 block effect was significant all along the survey, but higher at the end of the rotation. Residuals, i.e. the
498 part of the variance in stand growth not explained by these four variables, increased after 3 years of age.

499

500 4. Discussion

501

502 The *Eucalyptus* genotypes compared in our field trial were obtained from breeding programs located
503 throughout Brazil, and large difference in production dynamics was expected among them when planted
504 at a single location. The same planting date, stocking density and management practices over the study
505 area make it possible to assess the consequences of genotype choice and spatial variability of soil
506 resources on the dynamics of biomass accumulation in our field trial. The 10 blocks of the experiment
507 were indeed located close to each other, thus experiencing a similar climate while soil characteristics
508 substantially varied among blocks (Campoe *et al.*, 2012). The large range of productivity observed among
509 genotypes resulted in a valuable dataset for testing hypotheses on the effects of stand characteristics,
510 allometry and functional traits on productivity for several species and hybrids within the *Eucalyptus*
511 genus.

512 We observed that tree productivity was mainly driven by differences in genotypic performances. Indeed,
513 after excluding the plot of B4-G9 having very high mortality rate (Figure 6), the correlation between the
514 stem biomass of the most productive plots and the less productive plots among genotypes was high and
515 very significant ($r=0.90$ and $p<0.001$), which indicate that the most productive genotypes were
516 consistently more productive everywhere in the whole area despite the soil gradient. Most of the clonal
517 materials studied here had higher productivity than the two seed origin materials G1 and G2. To analyse
518 the productivity of each genotype, we followed the framework of the production ecology equation that
519 separates production into the product of resource supply, proportion of captured resource and efficiency
520 of resource use (Monteith and Moss, 1977). Light supply was considered equivalent for all plots of the
521 experiment, reducing the explained variation of productivity to variations of fAPAR and LUE for stem
522 wood production. LUE for stem wood production captures a variety of processes such as photosynthesis
523 per unit of absorbed light, which is function of the leaf photosynthetic characteristics and of the
524 environment, living biomass respiration, and partitioning of assimilated carbon to stemwood production
525 (Russell *et al.*, 1989).

526

527 *Variations of APAR, fAPAR and extinction coefficient with genotype and stand age*

528 Comparison between MAESTRA simulation and light interception measurements conducted *in situ*
529 showed strong adequacy (Supplementary Material 3). The model successfully predicted angular gap
530 fractions for all genotypes, i.e., it reproduced the absolute GF value in zenithal direction (mostly linked to
531 LAI) as well as the GF diminution with angle view (mostly linked to leaf angle and directional clumping).

532 fAPAR and APAR increased in the first two years after planting for all genotypes, before stabilizing at
533 fAPAR plateau values ranging from about 0.8 to 0.97 depending on the genotype. Similar dynamics of
534 fAPAR were observed in other studies, based on model simulations (le Maire *et al.*, 2013), or situ
535 measurements and remote sensing data (Marsden *et al.*, 2010). At all ages, genotypic differences in
536 fAPAR were driven by LAI (Table 3). For all genotypes, LAI increased rapidly after planting, reaching a
537 peak in the second or third year, and decreased afterward until the end of the rotation (Figure 4). This
538 typical age-related pattern in LAI has been reported for many *Eucalyptus* plantations across the world
539 (Ryan *et al.*, 2004; Whitehead and Beadle, 2004; du Toit, 2008; le Maire *et al.*, 2011). The decrease in
540 LAI toward the end of the rotation did not strongly affect fAPAR, since LAI values remained at high
541 levels for which the fAPAR vs. LAI relationships saturates. The genotypic variability in fAPAR was also
542 explained by LIA and crown sizes (Table 3). Crown size has an impact on the macro-clumping of LAI,
543 which was shown to enhance radiation transmission throughout the canopy and increase GPP (Rambal *et al.*,
544 2003). Although potentially contributing to inter-genotype differences in APAR, micro-clumping
545 inside tree crowns were not characterized in this study due to lack of data on the within-crown
546 distribution of leaves.

547 The integrated effect of changes in canopy structure on APAR was however captured in the extinction
548 coefficient k for daily PAR absorption (Equation 6, Figure 8 and Supplementary Material 4). Daily
549 extinction coefficients are useful for a simplified modelling of daily absorbed light from LAI and daily
550 incident PAR. The values of k estimated in the present study were in the 0.4 to 0.76 range. These values
551 are on the higher range of measured values reported in literature (Albaugh *et al.*, 2016). In the present
552 case, k estimated with MAESTRA considered the canopy properties, the course of the sun during the day
553 and the separation of direct and diffuse radiation. Extinction coefficient for diffuse sky radiation are
554 higher than for direct radiation, since extinction coefficients are lower at nadir when eventual direct PAR
555 is higher (Nouvellon *et al.*, 2000). On the contrary, diffuse extinction coefficient takes into account the
556 whole hemisphere, where nadir solid angles are under-represented compared to higher angles which have
557 higher directional k values. It underlines the necessity to distinguish the direct and diffuse radiation when
558 computing APAR (Li and Fang, 2015), as done in MAESTRA.

559 A decrease of the extinction coefficient between two and three years of age was also observed by Dovey
560 and Du Toit (2006), with lower values (from 0.55 to 0.42). Lower k values were obtained at LAI peak,
561 probably due to the decrease of diffuse extinction coefficient with LAI increase (Nouvellon *et al.*, 2000).
562 Differences between genotypes stayed along the rotation. Our results therefore showed that genotype- and
563 age-specific values of extinction coefficient are needed when using Equation (6) for computing fAPAR,

564 while most of modelling studies are using a default value of 0.5 (Landsberg and Hingston, 1996; Almeida
565 *et al.*, 2004; Pérez-Cruzado *et al.*, 2011).

566 Despite a rather simple representation of the 3D structure of canopies, other studies show that MAESTRA
567 is flexible enough to represent various types tree crowns, and fast enough to simulate APAR over entire
568 rotations (Bauerle *et al.*, 2004; Binkley *et al.*, 2010; Charbonnier *et al.*, 2013; Gspaltl *et al.*, 2013; le
569 Maire *et al.*, 2013). On the present study, MAESTRA accounted for variation of LIA at plot scale,
570 explaining large part of the APAR variation (Table 3). It confirmed that this variable should be
571 systematically estimated together with LAI when analysing *Eucalyptus* plantations APAR. Detailed
572 representation of specific tree traits such as vertical profiles of within-crown leaf inclination angles or leaf
573 area distribution would request more complex measurements and models, such as 3D structural models
574 describing each leaf orientation (Parveaud *et al.*, 2007). Gradient of inclination angles from erectophile on
575 the top to planophile on the bottom of the canopy is known as optimal for maximizing canopy
576 photosynthesis and limiting leaf photooxidative, temperature or water stresses associated with high
577 irradiance (Russell *et al.*, 1989; King, 1997; Posada *et al.*, 2009). Such optimality seems to be genotype-
578 dependent, and further studies are needed to examine the effect of LAI and leaf angles, together with
579 other variables such as SLA, nitrogen and photosynthetic parameters profiles on productivity. Leaf optical
580 properties were shown to have significant effect on fAPAR differences among genotypes. Correlation of
581 SPAD with PAR reflectance and transmittance observed in our dataset could facilitate the field estimation
582 of these characteristics. Finally, row orientation was accounted for in the MAESTRA simulation but its
583 effect on daily APAR and GPP was not studied here. A model such as DART (Gastellu-Etchegorry *et al.*,
584 2004), can help understanding further differences in light absorption regimes among genotypes and
585 locations, as was done in the same experiment in Oliveira *et al.* (2017).

586

587 *Variations of LUE with genotype and stand age*

588 The values of Light Use Efficiency for stemwood production obtained in the present study were in line
589 with measurements from previous studies led in *Eucalyptus* plantation in Brazil (Marsden *et al.*, 2010; le
590 Maire *et al.*, 2013), which showed similar patterns of strong increase at early age and saturation or
591 moderate increase after canopy closing. Light Use Efficiency is driven by a complex set of processes
592 ranging from leaf-scale to tree-scale levels (Binkley *et al.*, 2010) that need to be untangled to understand
593 the age-related trend observed in our trial. LUE and GE have different trends along the rotation, GE
594 showing less saturation due to increase of the APAR/LAI ratio after canopy closure. The photosynthetic
595 capacities of the leaves may change among genotypes and site conditions, but they were not measured in

596 this study. SPAD values averaged at stand scale, related to chlorophyll content (Pinkard *et al.*, 2006),
597 increased with tree age (Figure 8), but the link with photosynthetic capacity, and consequently LUE and
598 GE, is not straightforward and would require more investigations.

599 Gross photosynthesis can also be strongly impacted by drought periods, through changes in stomatal
600 conductance and eventually through leaf fall. There are large differences of leaf anatomy between these
601 genotypes, and sap flow measurements have also shown large differences in tree transpiration per unit of
602 leaf area in our experiment (unpublished data). Previous studies led in the same stand (Christina *et al.*,
603 2017) or in a close rainfall exclusion trial (Christina *et al.*, 2018) have shown that in this region,
604 *Eucalyptus* plantations established in deep sandy soils have access to important soil water stocks in the
605 first years after planting. Water stress therefore starts affecting plantation functioning and productivity
606 only after canopy closure at about 2 years of age. Our results suggest that this could also be the case for
607 most of the genotypes in the studied trial, but no measurements were made to confirm this hypothesis.

608 Partitioning of the photosynthesized carbon between respiration and allocation to tree organ is probably a
609 major driver of the changes in LUE with age, among genotypes and among sites. Indeed, partitioning is
610 predominantly oriented toward resource-capturing organs at the beginning of the rotation (especially the
611 first year) and toward woody organs latter in the rotation (Nouvellon *et al.*, 2012; Marsden *et al.*, 2013).
612 Shifts in carbon allocation with ontogeny, environmental constraints and resource availability was also
613 observed in Ryan *et al.* (2004) in another *Eucalyptus* genotype. Carbon partitioning to aboveground NPP
614 is also spatially variable: higher GPP and carbon partitioning to stemwood generally occurs in more
615 fertile sites (Haynes and Gower, 1995; Stape *et al.*, 2008; Campoe *et al.*, 2012; Vicca *et al.*, 2012).
616 Increasing soil nutrient availability can also enhance the carbon partition to aboveground tree components
617 (Giardina *et al.*, 2003; Litton *et al.*, 2007; Epron *et al.*, 2012). Water availability and stand structure also
618 alter carbon partitioning, e.g. between aboveground and belowground (Ryan *et al.*, 2004; Stape *et al.*,
619 2008).

620

621 *Effects of stand heterogeneity, tree mortality and soil properties on growth and LUE*

622 In general, mortality is low in commercial *Eucalyptus* plantation managed in short rotations, but it was
623 relatively high for some blocks and genotypes in our study as a result of tree fall after windy events,
624 lightning strikes, etc. Contrasting sensibilities of the 16 genotypes to wind and pathogens led to
625 significant differences in mortality rates. Mortality created or reinforced heterogeneity in tree size within
626 canopies by creating gaps. In this study, seed-origin plantations (G1 and G2) and clones G3 and G13
627 showed higher mortality rates. Heterogeneous canopies of *Eucalyptus* were shown to have lower

628 productivity (Binkley *et al.*, 2010; Ryan *et al.*, 2010; Stape *et al.*, 2010; Luu *et al.*, 2013). Similar
629 conclusions were found in monospecific European forests (Bourdier *et al.*, 2016). Here, the effect of stand
630 heterogeneity was assessed with two indices, the GINI index of tree basal areas and standard deviation of
631 height of living trees. Heterogeneity is especially high for seed-origins genotypes G1 and G2, which
632 probably reflects the heterogeneity of growth potential between seeds. Beyond biotic and abiotic mortality
633 events, the heterogeneity of clonal plantation is also the consequence of differences in the planting
634 conditions of each single tree. We observed that the GINI index of heterogeneity had a high and
635 significant effect on clone productivity (Figure 11).

636

637 *Contrasted light-use strategies among genotypes of the Eucalyptus genus*

638 A large diversity of trait combinations can be pointed out among the 16 highly productive genotypes in
639 our experiment. For example, some genotypes with contrasting profiles:

- 640 - G10 with high LAI and branch biomass, high LUE and GE, low mortality and heterogeneity
641 indices, strong growth at the end of the rotation in 5th and 6th years due to increase in LUE;
- 642 - G16 with low LAI and branch biomass, high leaf inclination angles, strong initial growth, low
643 heterogeneity indices, high LUE and GE at the beginning of the rotation but a clear slowing down
644 of LUE after 4 years, which result in a stem growth decline at the end of the rotation;
- 645 - G12 with low LAI and branch biomass, but high LUE and GE at the beginning but also at the end
646 of the rotation, which displayed high biomass at 6 years
- 647 - G2 with high intra-stand heterogeneity of growth, high mortality, high branch biomass but
648 average LAI, and lower LUE than average, which resulted in low standing biomass at 6 years

649

650 Such trait combinations show contrasting strategies for resource acquisition and growth. Our results
651 highlight the major importance of the two last years of the rotation to maximize the amount of stemwood
652 harvested at age 6 years. Indeed, the ranking of the genotypes changed substantially between the 4th and
653 5th year after planting (Figure 5). It underlines differences in resource acquisition dynamics and allocation
654 among genotypes of the *Eucalyptus* genus. This was confirmed by a mixed model which showed that the
655 final average stem biomass for each genotype was more closely explained by the average LUE of the 4th,
656 5th and 6th years (R^2 of 0.45, 0.64 and 0.61 respectively, all significant at $p < 0.01$) than by the LUE of the
657 previous years (correlation insignificant). The genotypes with the highest final biomass, such as G10 and
658 G12, were the ones with the highest final LUE.

659 An hypothesis to explain these differences is that after 3 years old, several factors start affecting
660 stemwood growth with different intensity among genotypes: water resource becomes a strong limiting
661 factor since all the annual rainfall (about 1500 mm) is used by the trees (Christina *et al.*, 2017), hydraulic
662 limitations may happen due to tree height (Ryan *et al.*, 2006), and tree height could enhance susceptibility
663 to wind damage. Other characteristics such as initial growth rates, stand homogeneity and APAR, were
664 not as important as LUE during the last years to explain stemwood biomass at harvest for our 16
665 genotypes. However, the diversity of growth patterns at the end of the rotation in our study is probably
666 influenced by the heterogeneity of the genotypes selected by forest companies from the South to the
667 North of Brazil. It underlines the fact that clonal selection is more reliable at harvesting age, which is
668 mostly the case in Brazil, but a more juvenile selection (around age 3 years) may still be valuable in forest
669 companies to rank less diverse genotypes adapted to specific climate and soil conditions.

670

671 An interesting trend, not analysed in details in the present study, is that genotypes having invested more
672 in leaves were generally more adapted to wet regions, such as G14 (*E. saligna* coming from a region
673 having mean daily temperature of 18.4°C, with 13.2-24.2°C range, and rainfall of ~1600 mm, Table 1),
674 while genotypes having lower LAI were more conservative for water use, such as G16 (*E. grandis* x *E.*
675 *camaldulensis* selected in a region having mean temperature of 24.7°C, with 22.4-26.1°C range and
676 rainfall of ~1000 mm). They also have contrasting investments in fine roots, which could results in
677 different abilities to access during dry periods to large amounts of water stored in the deep soil layers. In
678 our experiment, Pinheiro *et al.* (2016) have shown at age 2 years that the fine root biomass was different
679 between genotypes. The genotype with the highest fine root biomass, fine root length, and the maximum
680 depth reached by fine roots was the genotype with the lowest leaf area index. However, this investment in
681 fine roots at two years of age do not seem related to the final stemwood production at age 6 years, but the
682 four genotypes studied in Pinheiro *et al.* (2016) were among the genotypes with the lowest biomass at
683 harvest in our study (G1, G8, G14, G16). Modelling the differences of carbon cycling between genotypes
684 using process-based models would be useful to gain insight into the processes driving the changes in LUE
685 over the last years of the rotation.

686

687 **5. Conclusion**

688

689 As expected, the range of productivities was large in our study for *Eucalyptus* genotypes originating from
690 breeding programs located across a large climate gradient and grown in a single location. Productivity

691 was analysed here together with other characteristics of the stands, such as their leaf area index, level of
692 stand heterogeneity, and other functional traits. The genotypes showed large differences in dynamics of
693 LAI, APAR and in efficiency for using the absorbed APAR to grow wood. Differences of LAI and APAR
694 among genotypes were not linked to genotype productivity. Spatial variability of growth was directly
695 related to APAR for almost all genotypes the first two years after planting. Over the entire rotation, only 5
696 out of 16 genotypes showed significant correlation between total absorbed PAR and stemwood
697 production. The efficiency for converting radiation into stemwood is the major factor explaining i)
698 differences of productivity among genotypes, and ii) explaining differences of productivity of a given
699 genotype along a gradient of soil characteristic. LAI and LUE dynamics along the rotation were clone-
700 dependent. The LUE at the end of the rotation was the major factor differentiating the highly productive
701 from the less productive genotypes at age 6 years in monoclonal *Eucalyptus* plantations. The biological
702 mechanisms, and associated functional traits, that drive spatial and temporal changes of LUE in
703 commercial *Eucalyptus* plantations deserve closer attention.

704

705 **6. Acknowledgements**

706

707 This project was funded by the EUCFLUX project (cooperative program with Arcelor Mittal, Cenibra,
708 Bahia Specialty Cellulose, Duratex, Fibria, International Paper, Klabin, Suzano, and Vallourec Florestal),
709 coordinated by the Forestry Science and Eserach Institute - IPEF (<https://www.ipef.br/>). The experiment
710 also partially benefited of fundings from Agence Nationale de la Recherche (MACACC project ANR-13-
711 AGRO-0005, Viabilité et Adaptation des Ecosystèmes Productifs, Territoires et Ressources face aux
712 Changements Globaux AGROBIOSPHERE 2013 program) and the FAPESP-Microsoft Research project
713 SEMP (Process n. 2014/50715-9). The experimental site is part of the SOERE F-ORE-T, which is
714 supported annually by Ecofor, Allenvi and the French National Research Infrastructure ANAEE-F
715 (<http://www.anaee-france.fr/fr/>). We acknowledge support from the IN-SYLVA network. We are grateful
716 to the staff at the Itatinga Experimental Station, in particular Rildo Moreira e Moreira (Esalq, USP) and
717 Eder Araujo da Silva (<http://www.floragroapoio.com.br>) for their technical support. This project analyses
718 largely benefited from the Montpellier Bioinformatics Biodiversity (MBB) computing cluster platform
719 which is a joint initiative of laboratories within the CeMEB LabEx "Mediterranean Center for
720 Environment and Biodiversity", as part of the program "Investissements d'avenir" (ANR-10-LABX-
721 0004).

722

723 **7. References**

724

- 725 ABRAF, 2012. Chapter 01, Planted forests in Brazil. In, Statistical yearbook 2012.
726 Albaugh, T.J., Albaugh, J.M., Fox, T.R., Allen, H.L., Rubilar, R.A., Trichet, P., Loustau, D., Linder, S., 2016.
727 Tamm Review: Light use efficiency and carbon storage in nutrient and water experiments on major
728 forest plantation species. For Ecol Manag 376, 333-342.

729 Almeida, A.C., Landsberg, J.J., Sands, P.J., 2004. Parameterisation of 3-PG model for fast-growing
730 Eucalyptus grandis plantations. For Ecol Manag 193, 179-195.

731 Aspinwall, M.J., Pfautsch, S., Tjoelker, M.G., Vårhammar, A., Possell, M., Drake, J.E., Reich, P.B., Tissue,
732 D.T., Atkin, O.K., Rymer, P.D., Dennison, S., Van Sluyter, S.C., 2019. Range size and growth
733 temperature influence Eucalyptus species responses to an experimental heatwave. Global Change
734 Biology in press.

735 Battie-Laclau, P., Laclau, J.P., Domec, J.C., Christina, M., Bouillet, J.P., de Cassia Piccolo, M., de Moraes
736 Goncalves, J.L., e Moreira, R.M., Krusche, A.V., Bouvet, J.M., Nouvellon, Y., 2014. Effects of potassium
737 and sodium supply on drought-adaptive mechanisms in Eucalyptus grandis plantations. New Phytol
738 203, 401-413.

739 Bauerle, W.L., Bowden, J.D., McLeod, M.F., Toler, J.E., 2004. Modeling intra-crown and intra-canopy
740 interactions in red maple: assessment of light transfer on carbon dioxide and water vapor exchange.
741 Tree Physiol 24, 589-597.

742 Binkley, D., Campoe, O.C., Alvares, C., Carneiro, R.L., Cegatta, Í., Stape, J.L., 2017. The interactions of
743 climate, spacing and genetics on clonal Eucalyptus plantations across Brazil and Uruguay. For Ecol
744 Manag 405, 271-283.

745 Binkley, D., Laclau, J.-P., Sterba, H., 2013. Why one tree grows faster than another: Patterns of light use
746 and light use efficiency at the scale of individual trees and stands. For Ecol Manag 288, 1-4.

747 Binkley, D., Stape, J.L., Bauerle, W.L., Ryan, M.G., 2010. Explaining growth of individual trees: Light
748 interception and efficiency of light use by Eucalyptus at four sites in Brazil. For Ecol Manag 259, 1704-
749 1713.

750 Bourdier, T., Cordonnier, T., Kunstler, G., Piedallu, C., Lagarrigues, G., Courbaud, B., 2016. Tree Size
751 Inequality Reduces Forest Productivity: An Analysis Combining Inventory Data for Ten European
752 Species and a Light Competition Model. Plos One 11, e0151852.

753 Campoe, O.C., Stape, J.L., Laclau, J.P., Marsden, C., Nouvellon, Y., 2012. Stand-level patterns of carbon
754 fluxes and partitioning in a Eucalyptus grandis plantation across a gradient of productivity, in Sao
755 Paulo State, Brazil. Tree Physiol 32, 696-706.

756 Campoe, O.C., Stape, J.L., Nouvellon, Y., Laclau, J.-P., Bauerle, W.L., Binkley, D., Le Maire, G., 2013. Stem
757 production, light absorption and light use efficiency between dominant and non-dominant trees of
758 Eucalyptus grandis across a productivity gradient in Brazil. For Ecol Manag 288, 14-20.

759 Charbonnier, F., le Maire, G., Dreyer, E., Casanoves, F., Christina, M., Dauzat, J., Eitel, J.U.H., Vaast, P.,
760 Vierling, L.A., Roupsard, O., 2013. Competition for light in heterogeneous canopies: Application of
761 MAESTRA to a coffee (Coffea arabica L.) agroforestry system. Agric For Meteorol 181, 152-169.

762 Christina, M., Le Maire, G., Battie-Laclau, P., Nouvellon, Y., Bouillet, J.P., Jourdan, C., de Moraes
763 Goncalves, J.L., Laclau, J.P., 2015. Measured and modeled interactive effects of potassium deficiency
764 and water deficit on gross primary productivity and light-use efficiency in Eucalyptus grandis
765 plantations. Global Change Biology 21, 2022-2039.

766 Christina, M., le Maire, G., Nouvellon, Y., Vezy, R., Bordon, B., Battie-Laclau, P., Gonçalves, J.L.M.,
767 Delgado-Rojas, J.S., Bouillet, J.P., Laclau, J.P., 2018. Simulating the effects of different potassium and
768 water supply regimes on soil water content and water table depth over a rotation of a tropical
769 Eucalyptus grandis plantation. For Ecol Manag 418, 4-14.

770 Christina, M., Nouvellon, Y., Laclau, J.-P., Stape, J.L., Bouillet, J.-P., Lambais, G.R., le Maire, G., 2017.
771 Importance of deep water uptake in tropical eucalypt forest. Funct Ecol 31, 509-519.

772 Christina, M., Nouvellon, Y., Laclau, J.P., Stape, J.L., Campoe, O.C., le Maire, G., 2016. Sensitivity and
773 uncertainty analysis of the carbon and water fluxes at the tree scale in Eucalyptus plantations using a
774 metamodeling approach. Can J For Res 46, 297-309.

775 Cordonnier, T., Kunstler, G., 2015. The Gini index brings asymmetric competition to light. Perspectives in
776 Plant Ecology, Evolution and Systematics 17, 107-115.

777 Crous, J., Burger, L., Sale, G., 2013. Growth response at age 10 years of five Eucalyptus genotypes
778 planted at three densities on a drought-prone site in KwaZulu-Natal, South Africa. *Southern Forests:*
779 *a Journal of Forest Science* 75, 189-198.

780 Dovey, S., Du Toit, B., 2006. Calibration of LAI-2000 canopy analyser with leaf area index in a young
781 eucalypt stand.

782 Drake, J.E., Aspinwall, M.J., Pfautsch, S., Rymer, P.D., Reich, P.B., Smith, R.A., Crous, K.Y., Tissue, D.T.,
783 Ghannoum, O., Tjoelker, M.G., 2015. The capacity to cope with climate warming declines from
784 temperate to tropical latitudes in two widely distributed Eucalyptus species. *Global Change Biology*
785 21, 459-472.

786 du Toit, B., 2008. Effects of site management on growth, biomass partitioning and light use efficiency in
787 a young stand of Eucalyptus grandis in South Africa. *For Ecol Manag* 255, 2324-2336.

788 du Toit, B., Smith, C.W., Little, K.M., Boreham, G., Pallett, R.N., 2010. Intensive, site-specific silviculture:
789 Manipulating resource availability at establishment for improved stand productivity. A review of
790 South African research. *For Ecol Manag* 259, 1836-1845.

791 Elias, P., Boucher, D., 2014. Planting for the Future. How Demand for Wood Products Could Be Friendly
792 to Tropical Forests. In: Union of Concerned Scientists.

793 Epron, D., Laclau, J.P., Almeida, J.C., Goncalves, J.L., Ponton, S., Sette, C.R., Jr., Delgado-Rojas, J.S.,
794 Bouillet, J.P., Nouvellon, Y., 2012. Do changes in carbon allocation account for the growth response
795 to potassium and sodium applications in tropical Eucalyptus plantations? *Tree Physiol* 32, 667-679.

796 Epron, D., Nouvellon, Y., Mareschal, L., Moreira, R.M.e., Koutika, L.-S., Geneste, B., Delgado-Rojas, J.S.,
797 Laclau, J.-P., Sola, G., Gonçalves, J.L.d.M., Bouillet, J.-P., 2013. Partitioning of net primary production
798 in Eucalyptus and Acacia stands and in mixed-species plantations: Two case-studies in contrasting
799 tropical environments. *For Ecol Manag* 301, 102-111.

800 FAO, 2015. *Global Forest Resources Assessment 2015*.

801 Fernández-Tschieder, E., Binkley, D., 2018. Linking competition with Growth Dominance and production
802 ecology. *For Ecol Manag* 414, 99-107.

803 Forrester, D.I., Ammer, C., Annighöfer, P.J., Barbeito, I., Bielak, K., Bravo-Oviedo, A., Coll, L., del Río, M.,
804 Drössler, L., Heym, M., Hurt, V., Löf, M., den Ouden, J., Pach, M., Pereira, M.G., Plaga, B.N.E., Ponette,
805 Q., Skrzyszewski, J., Sterba, H., Svoboda, M., Zlatanov, T.M., Pretzsch, H., 2018. Effects of crown
806 architecture and stand structure on light absorption in mixed and monospecific Fagus sylvatica and
807 Pinus sylvestris forests along a productivity and climate gradient through Europe. *J Ecol* 106, 746-760.

808 Gastellu-Etchegorry, J.P., Martin, E., Gascon, F., 2004. DART: a 3D model for simulating satellite images
809 and studying surface radiation budget. *Int J Remote Sens* 25, 73-96.

810 Giardina, C.P., Ryan, M.G., Binkley, D., Fownes, J.H., 2003. Primary production and carbon allocation in
811 relation to nutrient supply in a tropical experimental forest. *Global Change Biology* 9, 1438-1450.

812 Gonçalves, J.L.d.M., Alvares, C.A., Higa, A.R., Silva, L.D., Alfenas, A.C., Stahl, J., Ferraz, S.F.d.B., Lima,
813 W.d.P., Brancalion, P.H.S., Hubner, A., Bouillet, J.-P.D., Laclau, J.-P., Nouvellon, Y., Epron, D., 2013.
814 Integrating genetic and silvicultural strategies to minimize abiotic and biotic constraints in Brazilian
815 eucalypt plantations. *For Ecol Manag* 301, 6-27.

816 Gonçalves, J.L.M., Wichert, M.C.P., Gava, J.L., Masetto, A.V., Junior, A.J.C., Serrano, M.I.P., Mello, S.L.M.,
817 2007. Soil fertility and growth of Eucalyptus grandis in Brazil under different residue management
818 practices. *Southern Hemisphere Forestry Journal* 69, 95-102.

819 Gspaltl, M., Bauerle, W., Binkley, D., Sterba, H., 2013. Leaf area and light use efficiency patterns of
820 Norway spruce under different thinning regimes and age classes. *For Ecol Manag* 288, 49-59.

821 Guillemot, J., Martin-StPaul, N.K., Dufrêne, E., François, C., Soudani, K., Ourcival, J.M., Delpierre, N.,
822 2015. The dynamic of the annual carbon allocation to wood in European tree species is consistent
823 with a combined source-sink limitation of growth: implications for modelling. *Biogeosciences* 12,
824 2773-2790.

825 Haynes, B.E., Gower, S.T., 1995. Belowground carbon allocation in unfertilized and fertilized red pine
826 plantations in northern Wisconsin. *Tree Physiol* 15, 317-325.

827 IBA, 2017. Brazilian Tree Industry Annual Report. [https://www.iba.org/datafiles/publicacoes/pdf/iba-](https://www.iba.org/datafiles/publicacoes/pdf/iba-relatorioanual2017.pdf)
828 [relatorioanual2017.pdf](https://www.iba.org/datafiles/publicacoes/pdf/iba-relatorioanual2017.pdf).

829 Keenan, R.J., Reams, G.A., Achard, F., de Freitas, J.V., Grainger, A., Lindquist, E., 2015. Dynamics of global
830 forest area: Results from the FAO Global Forest Resources Assessment 2015. *For Ecol Manag* 352, 9-
831 20.

832 King, D.A., 1997. The Functional Significance of Leaf Angle in *Eucalyptus*. *Aust J Bot* 45, 619-639.

833 Laclau, J.P., Almeida, J.C., Goncalves, J.L., Saint-Andre, L., Ventura, M., Ranger, J., Moreira, R.M.,
834 Nouvellon, Y., 2009. Influence of nitrogen and potassium fertilization on leaf lifespan and allocation
835 of above-ground growth in *Eucalyptus* plantations. *Tree Physiol* 29, 111-124.

836 Laclau, J.P., Bouillet, J.P., Goncalves, J.L.M., Silva, E.V., Jourdan, C., Cunha, M.C.S., Moreira, M.R., Saint-
837 Andre, L., Maquere, V., Nouvellon, Y., Ranger, J., 2008. Mixed-species plantations of *Acacia mangium*
838 and *Eucalyptus grandis* in Brazil - 1. Growth dynamics and aboveground net primary production. *For*
839 *Ecol Manag* 255, 3905-3917.

840 Landsberg, J.J., Hingston, F.J., 1996. Evaluating a simple radiation/dry matter conversion model using
841 data from *Eucalyptus globulus* plantations in Western Australia. *Tree Physiol* 16, 801-808.

842 Landsberg, J.J., Waring, R.H., 1997. A generalised model of forest productivity using simplified concepts
843 of radiation-use efficiency, carbon balance and partitioning. *For Ecol Manag* 95, 209-228.

844 le Maire, G., Marsden, C., Verhoef, W., Ponzoni, F.J., Lo Seen, D., Bégué, A., Stape, J.-L., Nouvellon, Y.,
845 2011. Leaf area index estimation with MODIS reflectance time series and model inversion during full
846 rotations of *Eucalyptus* plantations. *Remote Sens Environ* 115, 586-599.

847 le Maire, G., Nouvellon, Y., Christina, M., Ponzoni, F.J., Gonçalves, J.L.M., Bouillet, J.P., Laclau, J.P., 2013.
848 Tree and stand light use efficiencies over a full rotation of single- and mixed-species *Eucalyptus*
849 *grandis* and *Acacia mangium* plantations. *For Ecol Manag* 288, 31-42.

850 LI-Cor, I., 1992. LAI-2000 Plant Canopy Analyzer, Operating Manual. In. Lincoln, NE.

851 Li, W., Fang, H., 2015. Estimation of direct, diffuse, and total FPARs from Landsat surface reflectance
852 data and ground-based estimates over six FLUXNET sites. *Journal of Geophysical Research:*
853 *Biogeosciences* 120, 96-112.

854 Litton, C.M., Raich, J.W., Ryan, M.G., 2007. Carbon allocation in forest ecosystems. *Global Change*
855 *Biology* 13, 2089-2109.

856 Luu, T.C., Binkley, D., Stape, J.L., 2013. Neighborhood uniformity increases growth of individual
857 *Eucalyptus* trees. *For Ecol Manag* 289, 90-97.

858 Luyssaert, S., Inglima, I., Jung, M., Richardson, A., Reichstein, M., Papale, D., Piao, S.L., Schulze, E.-D.,
859 Wingate, L., Matteucci, G., Aragao, L., Aubinet, M., Beer, C., Bernhofer, C., Black, K., Bonal, D.,
860 Bonnefond, J.M., Chambers, J.Q., Ciais, P., Cook, B., Davis, K.J., Dolman, A.J., Gielen, B., Goulden,
861 M.L., Grace, J., Granier, A., Grelle, A., Griffis, T., Grünwald, T., Guidolotti, G., Hanson, P.J., Harding,
862 R., Hollinger, D.Y., Hutya, L.R., Kolari, P., Kruijt, B., Kutsch, W., Lagergren, F., Laurila, T., Law, B.E., Le
863 Maire, G., Lindroth, A., Loustau, D., Malhi, Y., Mateus, J., Migliavacca, M., Misson, L., Montagnani, L.,
864 Moncrieff, J., Moors, E.J., Munger, J.W., Nikinmaa, E., Ollinger, S.V., Pita, G., Rebmann, C., Rouspard,
865 O., Saigusa, N., Sanz, M.J., Seufert, G., Sierra, C., Smith, L.K., Tang, J., Valentini, R., Vesala, T.,
866 Janssens, I.A., 2007. CO₂ balance of boreal, temperate, and tropical forests derived from a global
867 database. *Global Change Biology* 13, 2509-2537.

868 MacDicken, K.G., 2015. Global Forest Resources Assessment 2015: What, why and how? *For Ecol Manag*
869 352, 3-8.

870 Marsden, C., Le Maire, G., Stape, J.L., Lo Seen, D., Rouspard, O., Cabral, O., Epron, D., Nascimento Lima,
871 A.M., Nouvellon, Y., 2010. Relating MODIS vegetation index time-series with structure, light

872 absorption and stem production of fast-growing Eucalyptus plantations. For Ecol Manag 259, 1741-
873 1753.

874 Marsden, C., Nouvellon, Y., Laclau, J.-P., Corbeels, M., McMurtrie, R.E., Stape, J.L., Epron, D., le Maire,
875 G., 2013. Modifying the G'DAY process-based model to simulate the spatial variability of *Eucalyptus*
876 plantation growth on deep tropical soils. For Ecol Manag 301, 112-128.

877 Monteith, J.L., Moss, C.J., 1977. Climate and the Efficiency of Crop Production in Britain [and Discussion].
878 Philosophical Transactions of the Royal Society of London. B, Biological Sciences 281, 277-294.

879 Nouvellon, Y., Begue, A., Moran, M.S., Lo Seen, D., Rambal, S., Luquet, D., Chehbouni, G., Inoue, Y.,
880 2000. PAR extinction in shortgrass ecosystems: effects of clumping, sky conditions and soil albedo.
881 Agric For Meteorol 105, 21-41.

882 Nouvellon, Y., Laclau, J.P., Epron, D., Le Maire, G., Bonnefond, J.M., Goncalves, J.L., Bouillet, J.P., 2012.
883 Production and carbon allocation in monocultures and mixed-species plantations of Eucalyptus
884 grandis and Acacia mangium in Brazil. Tree Physiol 32, 680-695.

885 Nouvellon, Y., Stape, J.L., Laclau, J.P., Bonnefond, J.M., Da Rocha, H.R., Campoe, O.C., Marsden, C.,
886 Bouillet, J.P., Loos, R.A., Kinana, A., Le Maire, G., Saint Andre, L., Roupsard, O., 2010. Water and
887 energy fluxes above an Eucalyptus plantation in Brazil: environmental control and comparison with
888 two eucalypt plantations in Congo. In, Sir Mark Oliphant Canopy Processes in a Changing Climate
889 Conference (formally the IUFRO Canopy Processes Meeting), Falls Creek, Victoria and Tarraleah,
890 Tasmania.

891 Nouvellon, Y., Stape, J.L., Le Maire, G., Bonnefond, J.-M., Guillemot, J., Christina, M., Bouillet, J.-P.,
892 Camargo Campoe, O., Laclau, J.-P., 2018. Full-rotation carbon, water and energy fluxes in a tropical
893 eucalypt plantation. In, Eucalyptus 2018. CIRAD, Montpellier, France, pp. 102-103, 101 poster.

894 Oliveira, J.D.C., Feret, J.B., Ponzoni, F.J., Nouvellon, Y., Gastellu Etchegorry, J.-P., Camargo Campoe, O.,
895 Stape, J.L., Estraviz Rodriguez, L.C., Le Maire, G., 2017. Simulating the canopy reflectance of different
896 eucalypt genotypes with the DART 3-D model. IEEE Journal of Selected Topics in Applied Earth
897 Observations and Remote Sensing 10, 4844-4852.

898 Pallett, R.N., Sale, G., 2004. The relative contributions of tree improvement and cultural practice toward
899 productivity gains in Eucalyptus pulpwood stands. For Ecol Manag 193, 33-43.

900 Parveaud, C.-E., Chopard, J., Dautzat, J., Courbaud, B., Auclair, D., 2007. Modelling foliage characteristics
901 in 3D tree crowns: influence on light interception and leaf irradiance. Trees 22, 87-104.

902 Payn, T., Carnus, J.-M., Freer-Smith, P., Kimberley, M., Kollert, W., Liu, S., Orazio, C., Rodriguez, L., Silva,
903 L.N., Wingfield, M.J., 2015. Changes in planted forests and future global implications. For Ecol Manag
904 352, 57-67.

905 Pérez-Cruzado, C., Muñoz-Sáez, F., Basurco, F., Riesco, G., Rodríguez-Soalleiro, R., 2011. Combining
906 empirical models and the process-based model 3-PG to predict Eucalyptus nitens plantations growth
907 in Spain. For Ecol Manag 262, 1067-1077.

908 Pfautsch, S., Harbusch, M., Wesolowski, A., Smith, R., Macfarlane, C., Tjoelker, M.G., Reich, P.B., Adams,
909 M.A., 2016. Climate determines vascular traits in the ecologically diverse genus Eucalyptus. Ecol Lett
910 19, 240-248.

911 Pinheiro, R.C., de Deus, J.C., Nouvellon, Y., Campoe, O.C., Stape, J.L., Aló, L.L., Guerrini, I.A., Jourdan, C.,
912 Laclau, J.-P., 2016. A fast exploration of very deep soil layers by Eucalyptus seedlings and clones in
913 Brazil. For Ecol Manag 366, 143-152.

914 Pinkard, E.A., Patel, V., Mohammed, C., 2006. Chlorophyll and nitrogen determination for plantation-
915 grown Eucalyptus nitens and E. globulus using a non-destructive meter. For Ecol Manag 223, 211-
916 217.

917 Pirard, R., Dal Secco, L., Warman, R., 2016. Do timber plantations contribute to forest conservation?
918 Environmental Science & Policy 57, 122-130.

919 Posada, J.M., Lechowicz, M.J., Kitajima, K., 2009. Optimal photosynthetic use of light by tropical tree
920 crowns achieved by adjustment of individual leaf angles and nitrogen content. *Ann Bot-London* 103,
921 795-805.

922 Rambal, S., Ourcival, J.-M., Joffre, R., Mouillot, F., Nouvellon, Y., Reichstein, M., Rocheteau, A., 2003.
923 Drought controls over conductance and assimilation of a Mediterranean evergreen ecosystem:
924 scaling from leaf to canopy. *Global Change Biol* 9, 1813-1824.

925 Reich, P.B., 2014. The world-wide 'fast-slow' plant economics spectrum: a traits manifesto. *J Ecol* 102,
926 275-301.

927 Resende, R.T., Marcatti, G.E., Pinto, D.S., Takahashi, E.K., Cruz, C.D., Resende, M.D.V., 2016. Intra-
928 genotypic competition of Eucalyptus clones generated by environmental heterogeneity can optimize
929 productivity in forest stands. *For Ecol Manag* 380, 50-58.

930 Resende, R.T., Soares, A.A.V., Forrester, D.I., Marcatti, G.E., dos Santos, A.R., Takahashi, E.K., e Silva, F.F.,
931 Grattapaglia, D., Resende, M.D.V., Leite, H.G., 2018. Environmental uniformity, site quality and tree
932 competition interact to determine stand productivity of clonal Eucalyptus. *For Ecol Manag* 410, 76-
933 83.

934 Rouspard, O., Dauzat, J., Nouvellon, Y., Deveau, A., Feintrenie, L., Saint-André, L., Mialet-Serra, I.,
935 Braconnier, S., Bonnefond, J.-M., Berbigier, P., Epron, D., Jourdan, C., Navarro, M., Bouillet, J.-P.,
936 2008. Cross-validating Sun-shade and 3D models of light absorption by a tree-crop canopy. *Agric For*
937 *Meteorol* 148, 549-564.

938 Russell, G., Jarvis, P., Monteith, J., 1989. Absorption of radiation by canopies and stand growth. *Plant*
939 *canopies: their growth, form and function* 31, 21-39.

940 Ryan, M.G., Binkley, D., Fownes, J.H., Giardina, C.P., Senock, R.S., 2004. An experimental test of the
941 causes of forest growth decline with stand age. *Ecol Monogr* 74, 393-414.

942 Ryan, M.G., Phillips, N., Bond, B.J., 2006. The hydraulic limitation hypothesis revisited. *Plant, Cell &*
943 *Environment* 29, 367-381.

944 Ryan, M.G., Stape, J.L., Binkley, D., Fonseca, S., Loos, R.A., Takahashi, E.N., Silva, C.R., Silva, S.R.,
945 Hakamada, R.E., Ferreira, J.M., Lima, A.M.N., Gava, J.L., Leite, F.P., Andrade, H.B., Alves, J.M., Silva,
946 G.G.C., 2010. Factors controlling Eucalyptus productivity: How water availability and stand structure
947 alter production and carbon allocation. *For Ecol Manag* 259, 1695-1703.

948 Sands, P.J., Landsberg, J.J., 2002. Parameterisation of 3-PG for plantation grown Eucalyptus globulus. *For*
949 *Ecol Manag* 163, 273-292.

950 Silva, P.H.M., Campoe, O.C., De Paula, R.C., Lee, D.J., 2016. Seedling Growth and Physiological Responses
951 of Sixteen Eucalypt Taxa under Controlled Water Regime. *Forests* 7, 110.

952 Soares, A.A.V., Leite, H.G., Souza, A.L., Silva, S.R., Lourenço, H.M., Forrester, D.I., 2016. Increasing stand
953 structural heterogeneity reduces productivity in Brazilian Eucalyptus monoclonal stands. *For Ecol*
954 *Manag* 373, 26-32.

955 Stape, J.L., Binkley, D., 2010. Insights from full-rotation Nelder spacing trials with Eucalyptus in São
956 Paulo, Brazil. *Southern Forests: a Journal of Forest Science* 72, 91-98.

957 Stape, J.L., Binkley, D., Ryan, M.G., 2008. Production and carbon allocation in a clonal Eucalyptus
958 plantation with water and nutrient manipulations. *For Ecol Manag* 255, 920-930.

959 Stape, J.L., Binkley, D., Ryan, M.G., Fonseca, S., Loos, R.A., Takahashi, E.N., Silva, C.R., Silva, S.R.,
960 Hakamada, R.E., Ferreira, J.M.d.A., Lima, A.M.N., Gava, J.L., Leite, F.P., Andrade, H.B., Alves, J.M.,
961 Silva, G.G.C., Azevedo, M.R., 2010. The Brazil Eucalyptus Potential Productivity Project: Influence of
962 water, nutrients and stand uniformity on wood production. *For Ecol Manag* 259, 1684-1694.

963 Vezy, R., Christina, M., Rouspard, O., Nouvellon, Y., Duursma, R., Medlyn, B., Soma, M., Charbonnier, F.,
964 Blitz-Frayret, C., Stape, J.-L., Laclau, J.-P., de Melo Virginio Filho, E., Bonnefond, J.-M., Rapidel, B., Do,
965 F.C., Rocheteau, A., Picart, D., Borgonovo, C., Loustau, D., le Maire, G., 2018. Measuring and

966 modelling energy partitioning in canopies of varying complexity using MAESPA model. *Agric For*
967 *Meteorol* 253-254, 203-217.

968 Vicca, S., Luyssaert, S., Peñuelas, J., Campioli, M., Chapin III, F.S., Ciais, P., Heinemeyer, A., Högberg, P.,
969 Kutsch, W.L., Law, B.E., Malhi, Y., Papale, D., Piao, S.L., Reichstein, M., Schulze, E.D., Janssens, I.A.,
970 2012. Fertile forests produce biomass more efficiently. *Ecol Lett* 15, 520-526.

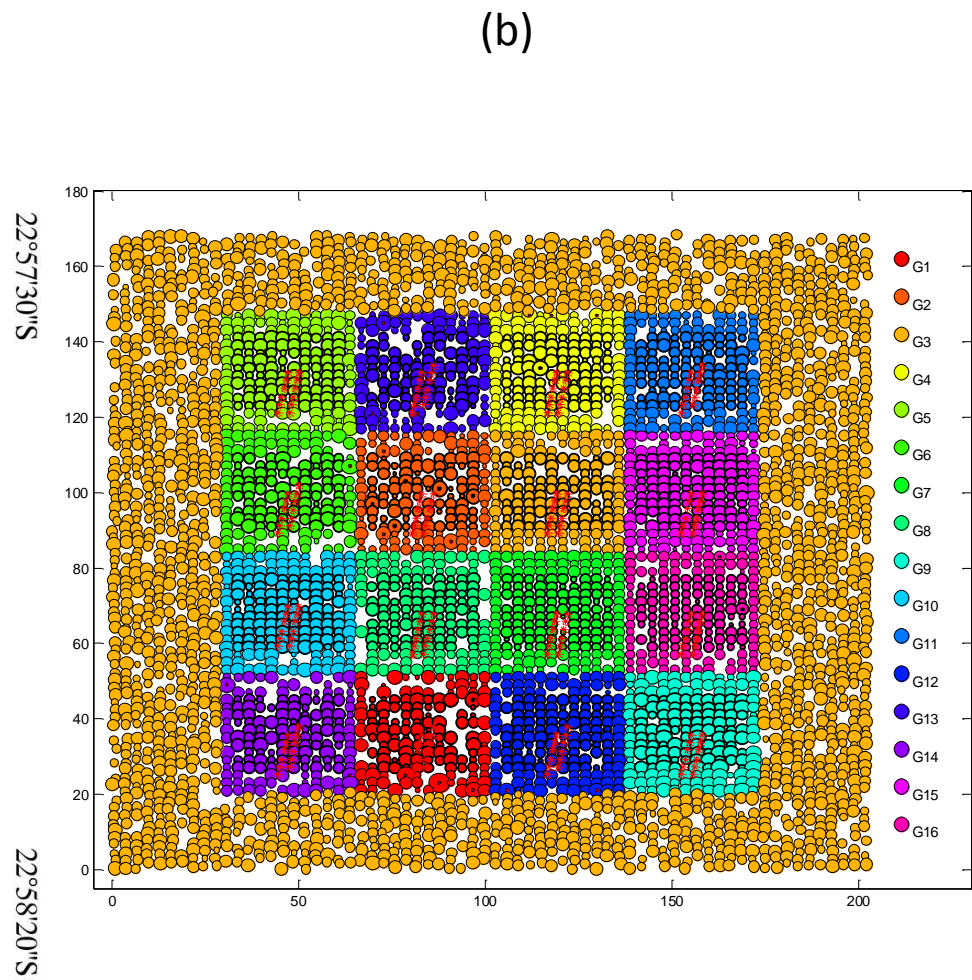
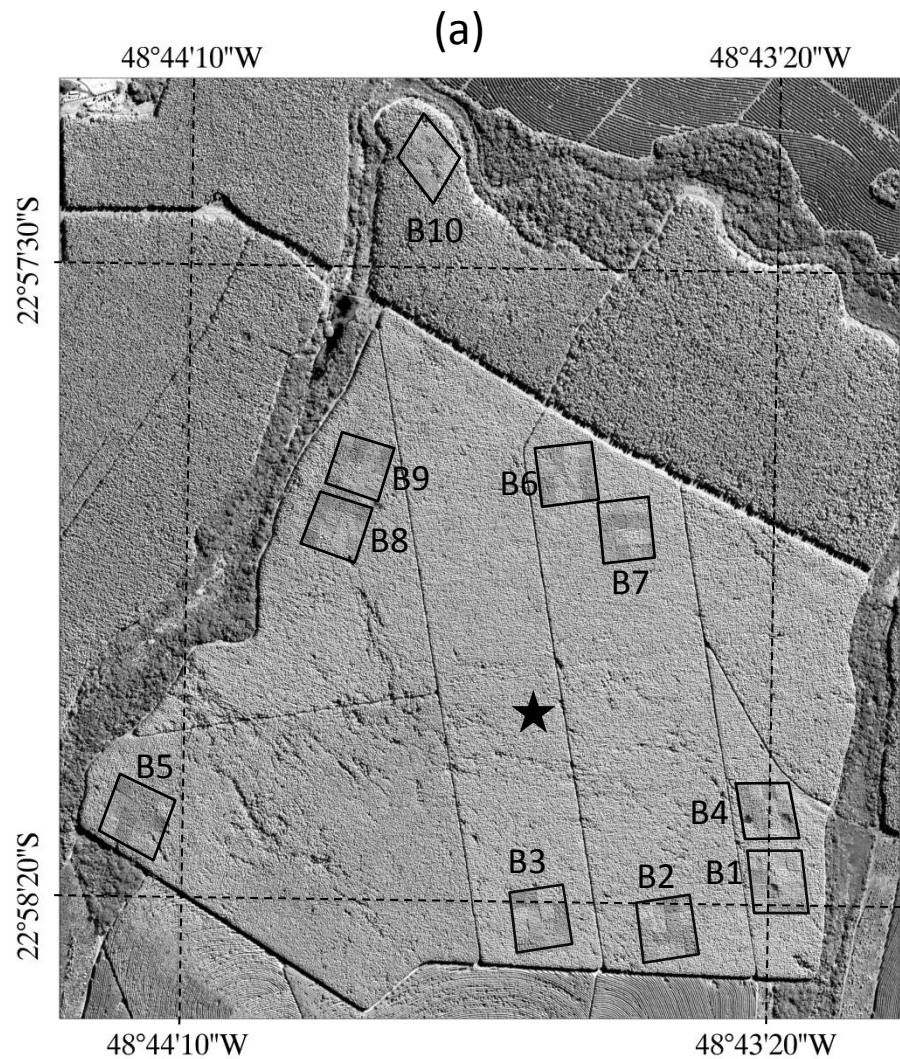
971 Wang, Y., Jarvis, P., Taylor, C., 1991. PAR absorption and its relation to above-ground dry matter
972 production of Sitka spruce. *J Appl Ecol*, 547-560.

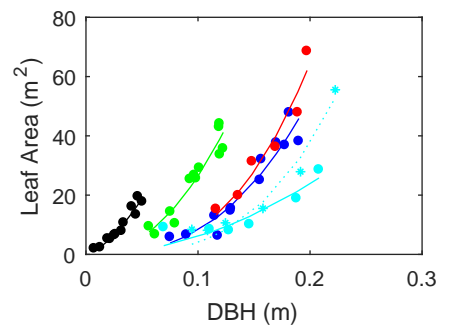
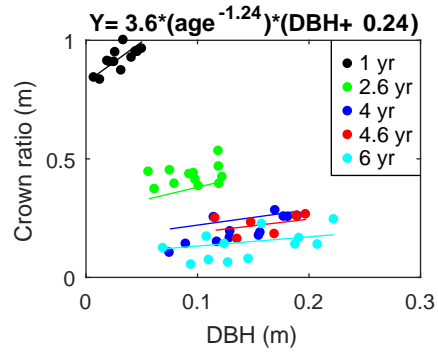
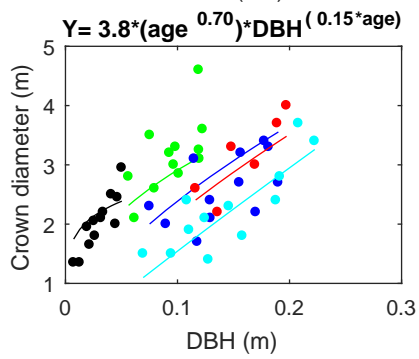
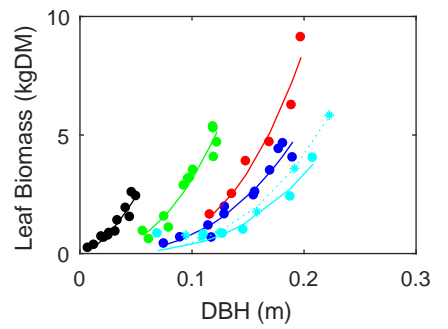
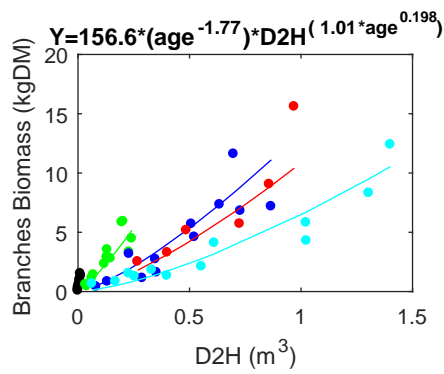
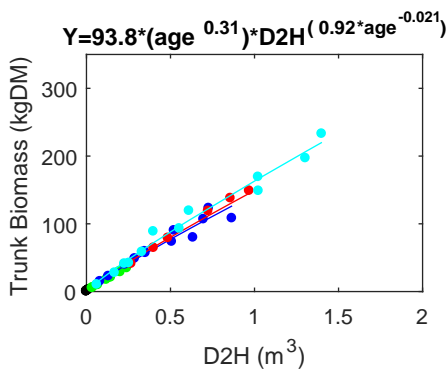
973 Whitehead, D., Beadle, C.L., 2004. Physiological regulation of productivity and water use in Eucalyptus: a
974 review. *For Ecol Manag* 193, 113-140.

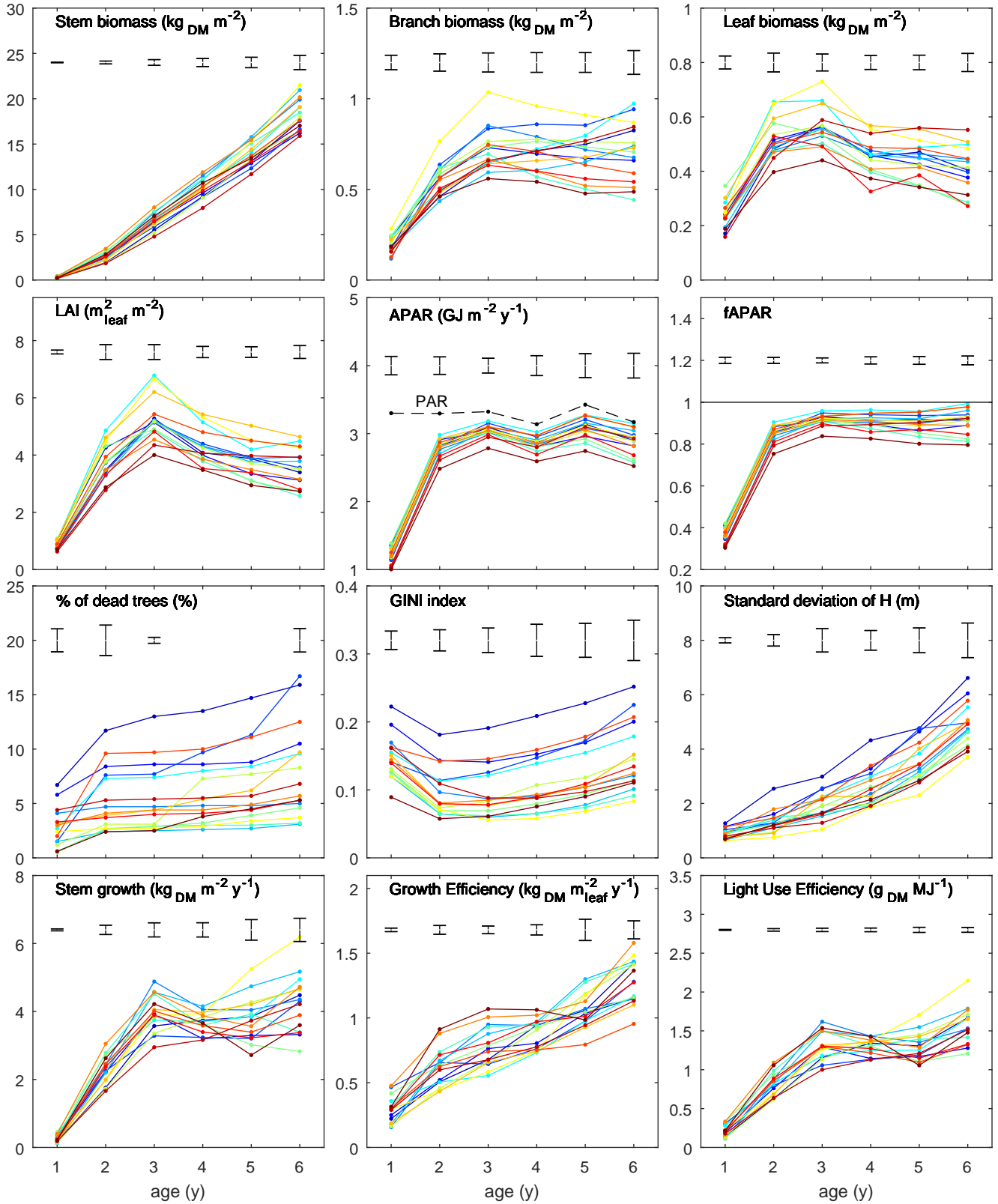
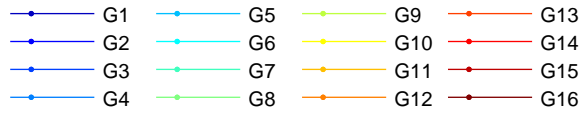
975 Will, R.E., Barron, G.A., Colter Burkes, E., Shiver, B., Teskey, R.O., 2001. Relationship between
976 intercepted radiation, net photosynthesis, respiration, and rate of stem volume growth of *Pinus*
977 *taeda* and *Pinus elliotii* stands of different densities. *For Ecol Manag* 154, 155-163.

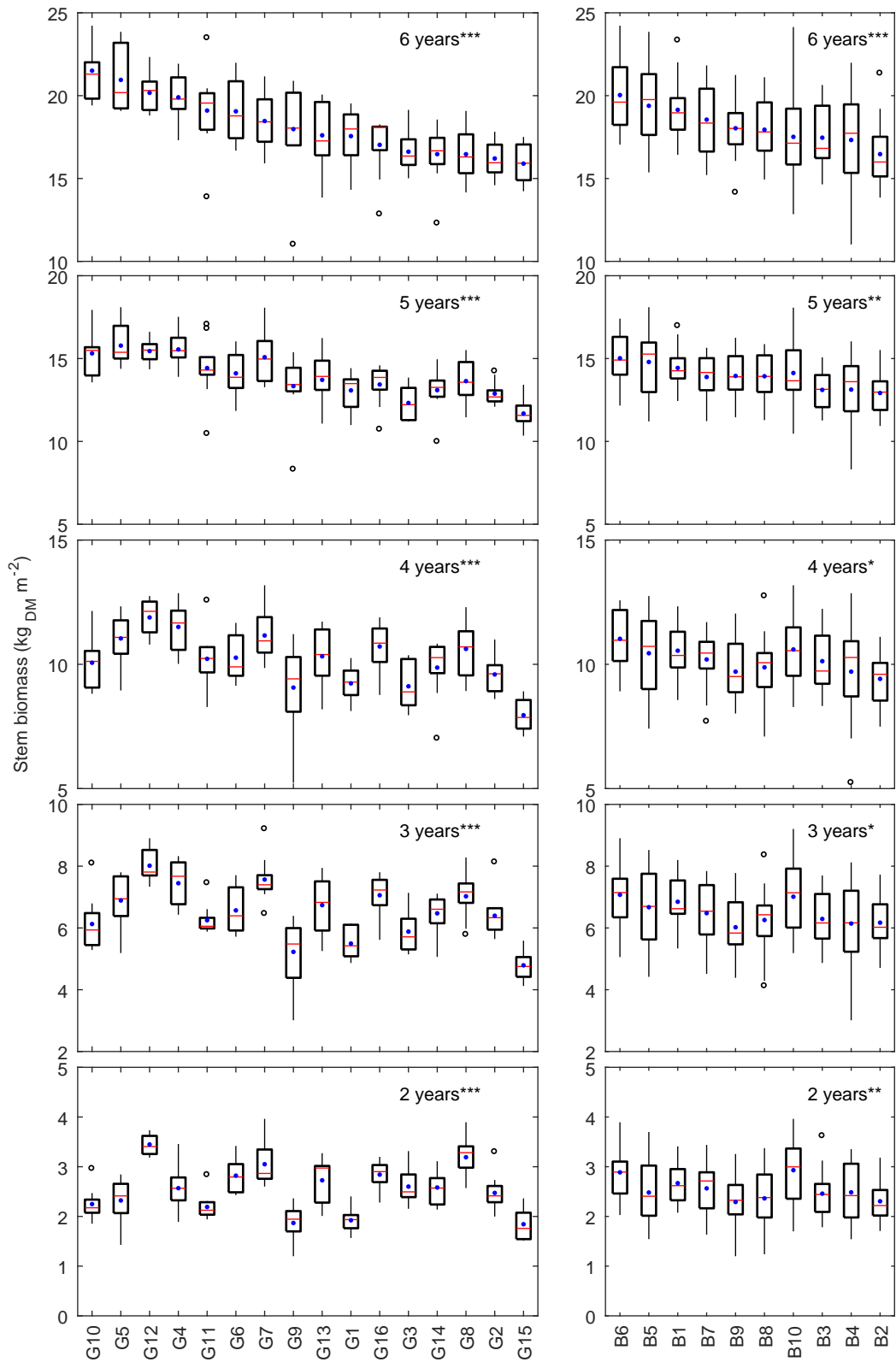
978

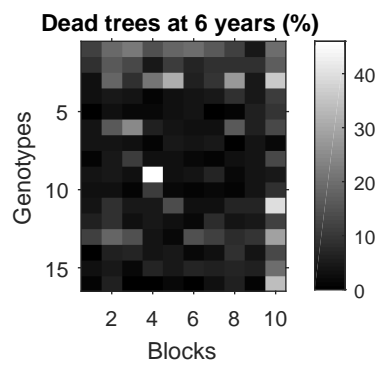
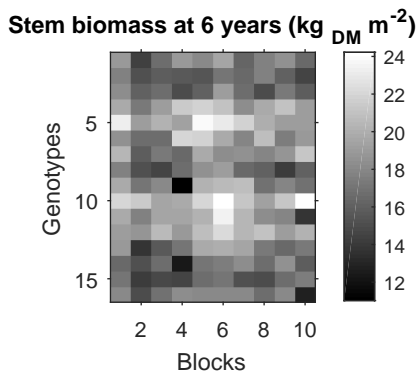
979

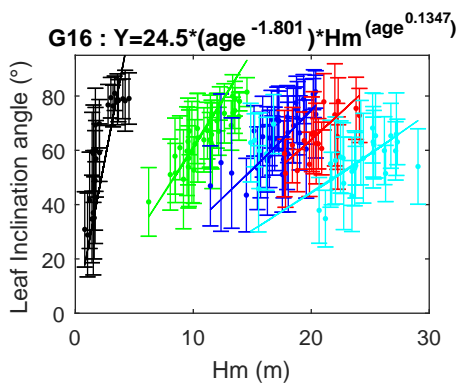
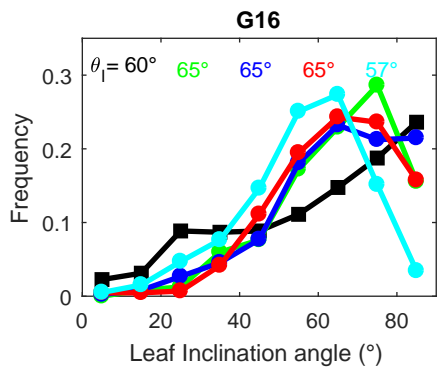
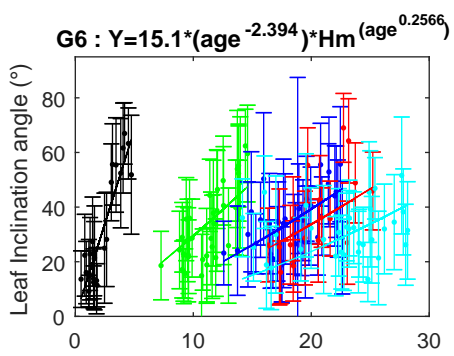
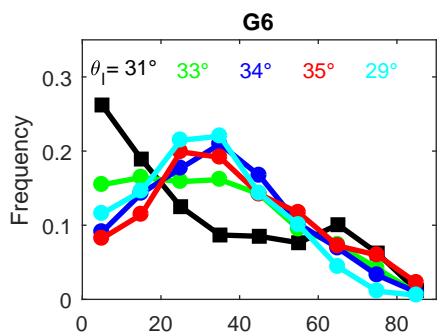


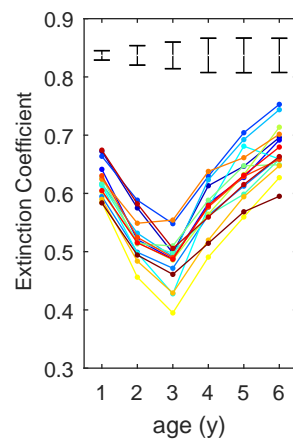
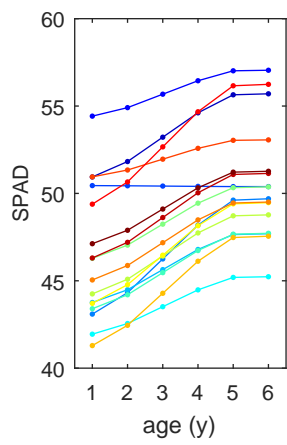


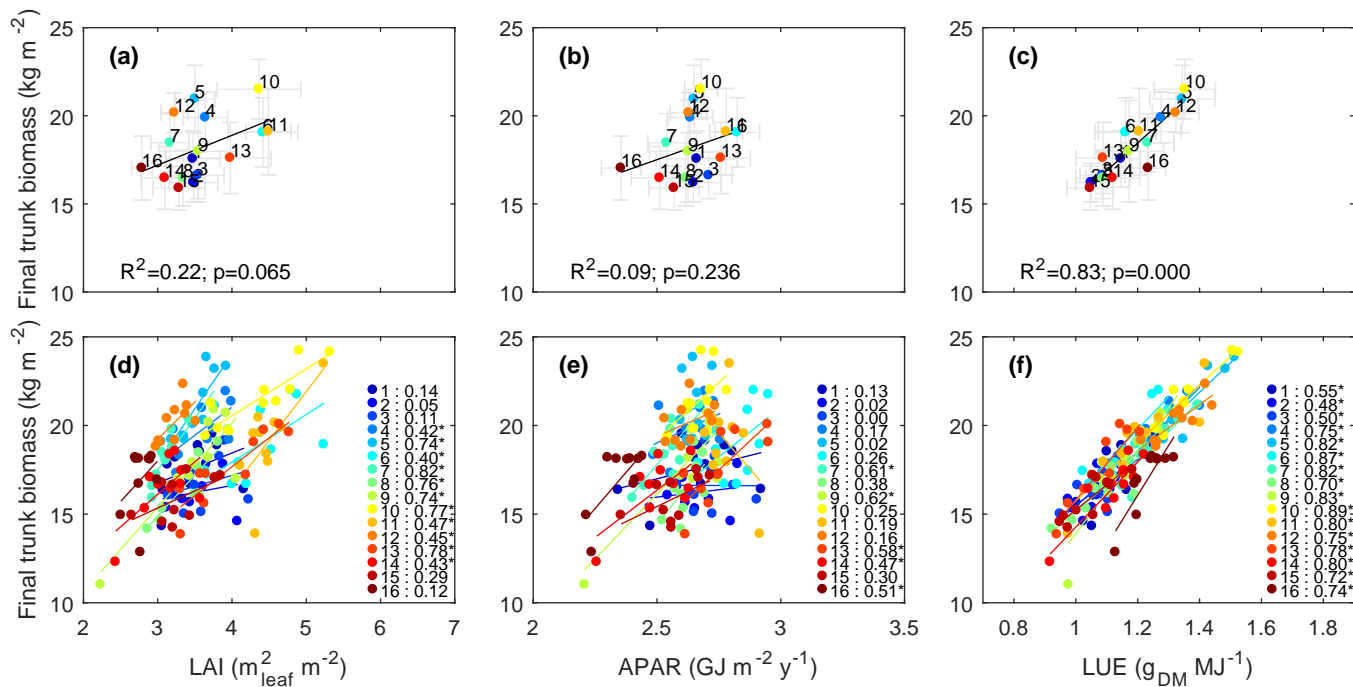


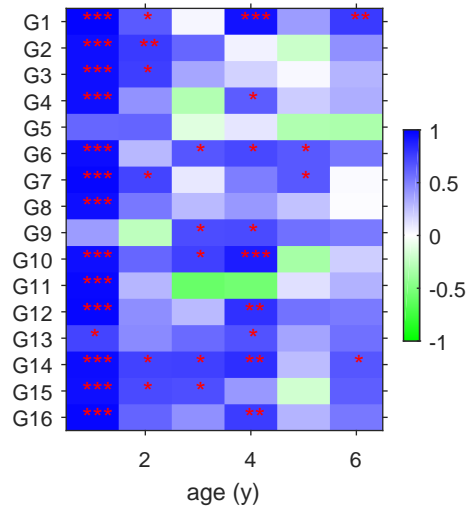












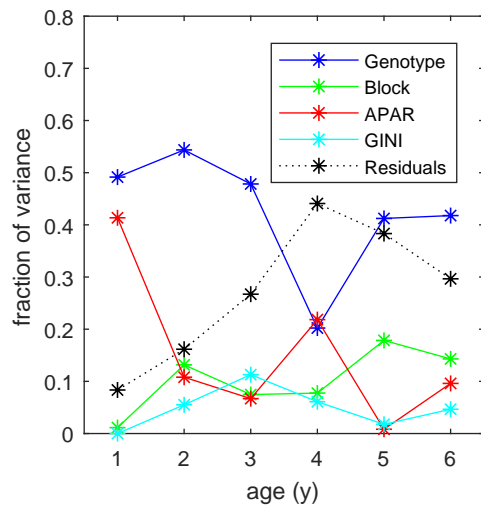


Table 1: Description of the 16 genotypes. Climate (annual mean) values are from (Alvares *et al.*, 2013). *States*: SP: são Paulo; ES: Espírito Santo; MG: Minas Gerais; BA: Bahia; RS: Rio Grande do Sul; *Climate*: Cfa: Humid subtropical zone without dry season and with hot summer; Cwa: Humid subtropical zone with dry winter and hot summer; Cfa: Humid subtropical zone without dry season and with hot summer; Aw: Tropical zone with dry winter; Am: Tropical zone – monsoon; Cwb: Humid subtropical zone with dry winter and temperate summer; As: Tropical zone with dry summer;

Genotype	Species	Propagation	State of origin	Climate	Minimum temperature (°C)	Maximum temperature (°C)	Mean annual temperature (°C)	Annual precipitation (mm)
1	<i>E. grandis</i>	Seed	SP	Cfa	15.9	22.5	19.7	1336
2	<i>E. grandis</i>	Seed	SP	Cfa	15.9	22.5	19.7	1336
3	<i>E. grandis</i> x <i>E. urophylla</i>	Clone	SP	Cwa	17.1	23.2	20.7	1463
4	<i>E. grandis</i> x <i>E. urophylla</i>	Clone	SP	Cfa	15.9	22.5	19.7	1336
5	<i>E. grandis</i> x <i>E. urophylla</i>	Clone	SP	Cwa	17.1	23.2	20.7	1463
6	<i>E. grandis</i> x <i>E. urophylla</i>	Clone	ES	Aw	20.2	26.1	23.4	1304
7	<i>E. grandis</i> x <i>E. urophylla</i>	Clone	MG	Cwa	17.9	22.9	21.1	1396
8	<i>E. grandis</i> x <i>E. urophylla</i>	Clone	MG	Aw	19.4	24.9	22.6	1370
9	<i>E. grandis</i> x <i>E. urophylla</i>	Clone	BA	Am	20.9	25.8	23.8	1192
10	<i>E. grandis</i> x <i>E. urophylla</i>	Clone	SP	Cfa	15.4	22.4	19.3	1245
11	<i>E. grandis</i> x <i>E. urophylla</i>	Clone	SP	Cfa	15.4	22.4	19.3	1245
12	<i>E. urophylla</i> x <i>sp</i>	Clone	MG	Cwb	16.5	21.7	19.7	1180
13	<i>E. grandis</i> x <i>E. urophylla</i>	Clone	MG	Cwb	16.5	21.7	19.7	1180
14	<i>E. saligna</i>	Clone	RS	Cfa	13.2	24.2	18.4	1594
15	<i>E. grandis</i>	Clone	SP	Cfa	15.4	22.4	19.3	1245
16	<i>E. grandis</i> x <i>E. camaldulensis</i>	Clone	BA	As	22.4	26.1	24.7	1045

Alvares, A.C., Stape, J., Sentelhas, P., Gonçalves, J., Sparovek, G., 2013. Köppen's climate classification map for Brazil.

Table 2: Description of the measurements conducted in the experiment. Each number is a code described below the table, informing on the measured blocks and genotypes numbers. Other information such as the number of trees or leaves sampled are also given. DBH: trunk diameter at 1.3 m; Refl/Tran: reflectance/transmittance; LAI-2000: measurements with the LiCor PCA LAI-2000 device (see section 2.6).

Date	age (years)	DBH	H	DBH border t.	Biomass	Leaf angles	SPAD	Leaf Refl/Tran	LAI-2000
03/11/2009	0								
17/05/2010	0.53	1	1						
03/11/2010	1.00	1	1		5a	6	7	7	
01/06/2011	1.58	1	1						
01/01/2012	2.16	1	1						
01/06/2012	2.58			4	5a	6			
01/07/2012	2.66	3	3						
15/01/2013	3.20	1	2						
15/07/2013	3.70	3	3						
15/11/2013	4.04				6b	6b			
15/02/2014	4.29	1	2						
15/06/2014	4.62								9
23/06/2014	4.64	3	3	4	5b	6	8		
31/10/2014	5.00	3b	3b						
15/02/2015	5.28	1	2						
15/07/2015	5.70	3	3						
15/11/2015	6.03				5b	6	7	7	
15/01/2016	6.20	1	2						

1: all blocks; all genotypes; all inside plot trees	6: B2 B3 B10; all genotypes; 12 trees/genotype; 60 leaves/tree
2: all blocks; all genotypes; 24 inside plot trees/genotype	6b: B2 B3 B10; G1 G6 G8 G12 G14 G16; 12 trees/genotype; 60 leaves/tree
3: B3 B8 B10; G1 G6 G8 G12 G14 G16; all inside plot trees	7: B1 B2; all genotypes; 3 trees/genotype; 6 leaves/tree
3b: B3 B8 B10; G1 G6 G8 G12 G14 G16; 24 inside plot trees/genotype	8: B2 B3 B10; all genotypes; 3 trees/genotype; 6 leaves/tree
4: all blocks; all genotypes; all border trees	9: B2 B3 B8; all genotypes; 12 positions/genotype
5a: B1 B2 B4 B5 B6 B7 B9 ; all genotypes; 6-12 trees/genotype	
5b: B2 B3 B8 B10 ; all genotypes; 6-12 trees/genotype	

Table 3: Result of mixed model of fAPAR in function of plot averages characteristics, with all genotypes included and with the blocks considered as random effect. One model was adjusted each year. Some variables, noted “o”, were first removed after computing their Variance Inflation Factors (VIF), to solve multicollinearity issue (see Section 2.7). Then, a backward elimination of non-significant effects of the linear mixed effects model was performed (eliminated variables are noted “x”). Remaining significant variables are labelled with *** if $p < 0.001$, ** $p < 0.01$, * $p < 0.05$ of the F-test of the fixed effects, green if the effect on fAPAR is positive and red if the effect is negative

Age	1	2	3	4	5	6
LAI	***	***	***	***	***	***
LIA	***	***	***	***	o	o
Reflectance	x	*	x	o	x	*
Transmittance	x	x	*	x	***	***
SPAD	o	***	x	x	***	x
Crown height	o	o	o	o	o	o
Crown diameter	***	o	o	o	***	***
Crown volume	o	***	x	x	o	o
Crown ratio	o	x	*	**	*	*
Trunk biomass	x	***	o	x	o	x
H	***	o	***	***	***	***
DBH	o	o	x	o	*	**
GINI	x	x	o	o	o	o
Mortality	x	x	x	***	x	x